


## RESEARCH ARTICLE

# Egomotion-related visual areas respond to active leg movements

Chiara Serra<sup>1,2</sup> | Claudio Galletti<sup>3</sup> | Sara Di Marco<sup>1,2</sup> | Patrizia Fattori<sup>3</sup> |  
Gaspare Galati<sup>2,4</sup> | Valentina Sulpizio<sup>3</sup> | Sabrina Pitzalis<sup>1,2</sup> 

<sup>1</sup>Department of Movement, Human and Health Sciences, University of Rome "Foro Italico", Rome, Italy

<sup>2</sup>Department of Cognitive and Motor Rehabilitation and Neuroimaging, Santa Lucia Foundation (IRCCS Fondazione Santa Lucia), Rome, Italy

<sup>3</sup>Department of Biomedical and Neuromotor Sciences, University of Bologna, Bologna, Italy

<sup>4</sup>Brain Imaging Laboratory, Department of Psychology, Sapienza University, Rome, Italy

## Correspondence

Sabrina Pitzalis, Department of Movement, Human and Health Sciences, University of Rome Foro Italico, 00194 Rome, Italy.  
Email: sabrina.pitzalis@uniroma4.it

## Funding information

PRIN, Grant/Award Number: 2015AWSW2Y; The University of Foro Italico, Grant/Award Number: CDR2.FFABR

## Abstract

Monkey neurophysiology and human neuroimaging studies have demonstrated that passive viewing of optic flow stimuli activates a cortical network of temporal, parietal, insular, and cingulate visual motion regions. Here, we tested whether the human visual motion areas involved in processing optic flow signals simulating self-motion are also activated by active lower limb movements, and hence are likely involved in guiding human locomotion. To this aim, we used a combined approach of task-evoked activity and resting-state functional connectivity by fMRI. We localized a set of six egomotion-responsive visual areas (V6+, V3A, intraparietal motion/ventral intraparietal [IPSmot/VIP], cingulate sulcus visual area [CSv], posterior cingulate sulcus area [pCi], posterior insular cortex [PIC]) by using optic flow. We tested their response to a motor task implying long-range active leg movements. Results revealed that, among these visually defined areas, CSv, pCi, and PIC responded to leg movements (visuomotor areas), while V6+, V3A, and IPSmot/VIP did not (visual areas). Functional connectivity analysis showed that visuomotor areas are connected to the cingulate motor areas, the supplementary motor area, and notably to the medial portion of the somatosensory cortex, which represents legs and feet. We suggest that CSv, pCi, and PIC perform the visual analysis of egomotion-like signals to provide sensory information to the motor system with the aim of guiding locomotion.

## KEYWORDS

brain mapping, CSv, functional connectivity, locomotion, optic flow, self-motion

## 1 | INTRODUCTION

The neural bases of visual motion perception have always received great attention in neuroscience field. In particular, a peculiar aspect of visual motion experience, the cortical mechanisms of self-motion (or egomotion) perception, has been repeatedly addressed by different laboratories. Optic flow constitutes a rich source of essential visual cues for the estimation of self-motion (egomotion; Gibson, 1950) and for facilitating navigation (i.e., locomotion) through the external environment (Bremmer, 2011; Marigold, 2008; Rushton, Niehorster, Warren, & Li, 2018); hence, it has been typically used to

study the cortical mechanisms of egomotion perception. Monkey neurophysiology and human neuroimaging studies have demonstrated that passive viewing of optic flow stimuli activates several higher level motion areas, including the medial superior temporal area (MST; Duffy, 1998, Dukelow et al., 2001), the ventral intraparietal area (VIP; Duhamel, Colby, & Goldberg, 1998; Bremmer et al., 2001; Sereno & Huang, 2006), the posterior insular cortex (PIC or visual posterior sylvian area; Cardin & Smith, 2010; Chen, DeAngelis, & Angelaki, 2011a, Frank, Baumann, Mattingley, & Greenlee, 2014; Cottureau et al., 2017), the lateral intraparietal sulcus (IPS, Cottureau et al., 2017; Pitzalis et al., 2010; Sereno, Pitzalis, & Martinez, 2001), and the

cingulate sulcus visual area (CSv; Wall & Smith, 2008; Cardin & Smith, 2010; Cottureau et al., 2017). In humans, responses to optic flow have been also found in the medial parieto-occipital areas V6 and V6Av (V6 complex or V6+; Pitzalis et al., 2006, 2010; Pitzalis, Sereno, et al., 2013; Cardin & Smith, 2010), in the precuneate area (Pc; Cardin & Smith, 2010), and, although less consistently, in other areas as the human homologous of the macaque vestibular area 2v (putative 2v or p2v; Guldin & Grüsser, 1998; Cardin & Smith, 2010) and the lateral occipitotemporal MT complex (MT+; Cardin & Smith, 2010).

Although all these regions highly respond to optic flow, or to egomotion-compatible visual stimuli as those used by Cardin and Smith (2010), they show many differences in terms of retinotopic organization and functional properties. Indeed, these regions cover a large cortical territory including temporal, parietal, insular, and cingulate regions (for a review, see Greenlee et al., 2016). Some of them (e.g., V6+, VIP, V3A, MT+, and MST) are more clearly retinotopically organized (e.g., Kolster, Peeters, & Orban, 2010; Pitzalis et al., 2006, 2010; Sereno & Huang, 2006; Tootell et al., 1997). Responses to changing heading directions were markedly found only in PIC (Huang, Chen, & Sereno, 2015), VIP, and CSv (Furlan, Wann, & Smith, 2014). V6+ and VIP are specialized in distinguishing among different types of self-movement, showing a strong response to translational egomotion (Pitzalis, Sdoia, et al., 2013). VIP and PIC also show vestibular responses and appear to integrate visual and vestibular cues to estimate self-motion (e.g., Billington & Smith, 2015; Greenlee et al., 2016; Smith et al., 2012; Smith, Greenlee, DeAngelis, & Angelaki, 2017). Finally, it has been suggested that some dorsal motion areas (like V3A and V6) likely contribute to perceptual stability during pursuit eye movements (Fischer, Bühlhoff, Logothetis, & Bartels, 2012a; Galletti, Battaglini, & Fattori, 1990; Galletti & Fattori, 2003) and could be involved in the “flow parsing” mechanism, that is the capability to extract object motion information from retinal motion signals by subtracting out the optic flow components (Warren & Rushton, 2009).

Overall, macaque and human results reviewed above suggest that the neural substrates of egomotion perception raise from a distributed and integrated network, involving early and higher order regions having different functional properties. In addition, some recent findings are in support of a diverse pattern of cortical connections of these areas. For example, it has been recently found that area CSv is connected to most anterior motor and somatosensory medial areas (Smith, Beer, Furlan, & Mars, 2017), which represent the legs and feet, suggesting a role in guiding locomotion. However, no studies so far have tested the response of area CSv to a motor task involving legs and feet movements. Since Tosoni et al. (2015) have recently reported that the visual area V6+ is mainly connected with posterior, visual regions of the brain (as MT+ and V1), one possible hypothesis is that the posterior egomotion areas (such as V6+) only contribute to the visual analysis of egomotion signals, while the anterior egomotion areas (such as CSv), closer to the somatosensory and motor areas, provide sensory information to the motor system with the aim of guiding locomotion.

To test this hypothesis, we used task-evoked fMRI to localize a set of egomotion-related areas using the flow field stimulus (e.g., Pitzalis et al., 2010) which produces patterns of coherent motion stimulation

similar to the continuously changing optic flow generated when a person moves through a complex environment (Koenderink & Physics, 1986). Specifically, we mapped the position of areas V6+, V3A, CSv, pCi, PIC, and a parietal region corresponding to the human VIP functionally defined by Cardin and Smith (2010) but given the homology uncertainty about human VIP (see also Pitzalis, Sdoia, et al., 2013), we hereafter call this parietal region intraparietal motion (IPSmot/VIP).

We tested the sensitivity of these areas to a pure motor task requiring to actively perform long-range leg and arm movements. We expected that the regions specialized in the motor control of locomotion are effector selective, responding more to leg than arm movements, being the legs, the effectors used for moving into the environment. Finding visually mapped egomotion areas that respond to active leg but not arm movements would suggest their direct role in human locomotion, a role so far only suggested based on the pattern of cortical connections (e.g., Smith, Beer, et al., 2017).

Finally, we examined the pattern of functional cortical connections, as estimated through resting-state functional connectivity MRI (fcMRI), of all egomotion-sensitive areas. We hypothesized that if an area plays a role in the motor control during locomotion, then this region should be functionally connected with the medial part of somatosensory and motor areas (where feet and legs are represented).

## 2 | METHODS

### 2.1 | Subjects

Eighteen healthy adults participated in the study (mean age 26 years,  $SD = 6.08$ , 11 females). All participants had normal or corrected-to-normal vision and no previous history of psychiatric or neurologic disease. All subjects were right-handed and right-footed, as assessed by the Edinburgh handedness inventory (Oldfield, 1971). All subjects gave written informed consent in accordance with guidelines set by the local Ethics Committee of Fondazione Santa Lucia, Rome, Italy.

### 2.2 | Stimuli and experimental paradigm

Participants laid on their back in the scanner. Each participant completed in different sessions three sets of fMRI scans: (a) a series of scans consisting of a visual stimulation paradigm, hereafter called either visual motion task or flow fields (Figure 1a), which we have previously proposed as a functional localizer for human V6+ (Pitzalis et al., 2010); (b) a series of scans consisting of active upper and lower limb movement task, hereafter called motor task (Figure 1b,c), designed to maximally activate leg and arm movement-related cells; and (c) a series of resting-state scans to evaluate intrinsic functional connectivity, in which subjects were lying at rest with eyes closed and no experimenter-imposed task.

#### 2.2.1 | Visual motion task

The flow field stimulus was described in detail in Pitzalis et al. (2010) and it is currently used in our laboratory as the localizer of area V6+

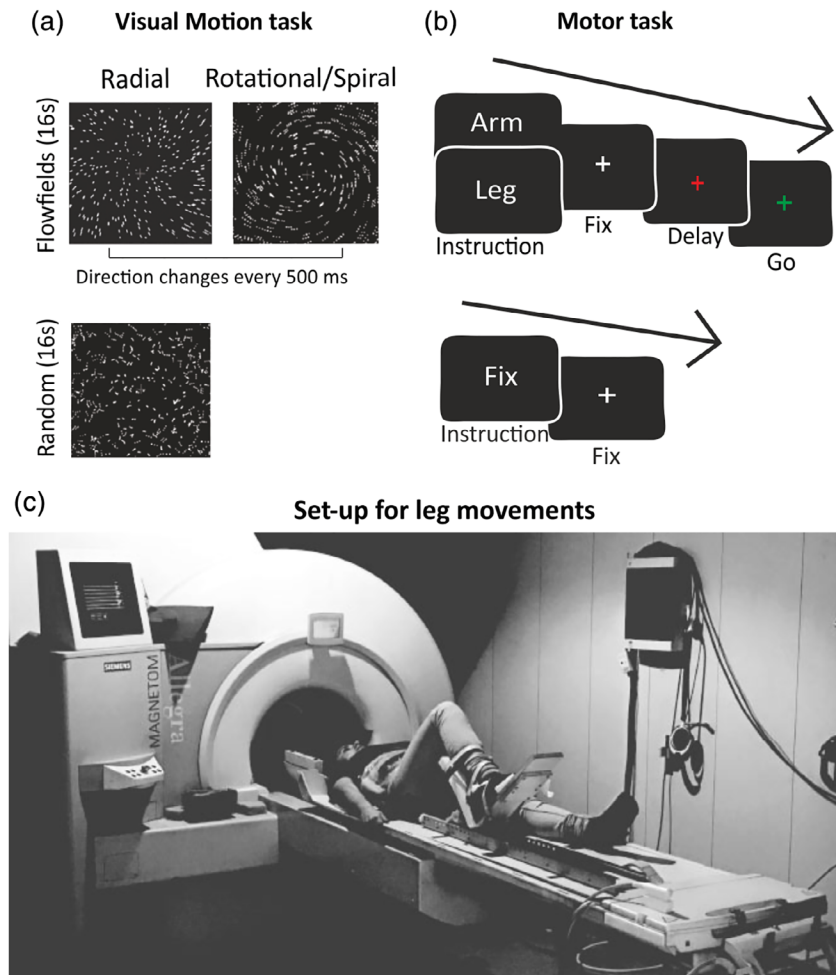


**FIGURE 1** Experimental tasks and setup. (a) Visual motion task. Blocks of coherently moving dot fields (flow fields) were interleaved with blocks of randomly moving dot fields. (b) Motor task. Participants alternated blocks of instructed long-range arm or leg movements with blocks of passive fixation. (c) A subject lying supine in the MRI scanner and performing a long-range leg movement during the motor task by using the experimental setup for leg movements [Color figure can be viewed at [wileyonlinelibrary.com](http://wileyonlinelibrary.com)]

(Figure 1). Briefly, participants were instructed to maintain central fixation while presented with four 16-s blocks of coherently moving dot fields (dilations, contractions, spirals, and rotations) interleaved with four 16-s blocks of randomly moving dot fields. A new field of white dots was generated every 500 ms (total number of dots = 2,000). The average luminance of the stimulus was  $31 \text{ cd/m}^2$ . Subjects reported that the visual motion task produced a compelling illusory perception of self-motion (vection).

### 2.2.2 | Motor task

Each scan consisted of seven arm and seven leg movement blocks lasting 20.5 s each, arranged in a pseudorandom sequence and interleaved with 14 fixation periods of variable duration (12, 14, or 16 s). At the beginning of each block, a written instruction (“FIX,” “LEG,” or “ARM”) appeared for 400 ms at the center of the screen to inform on the task to be performed. During fixation blocks, subjects were asked only to maintain fixation throughout the block. In leg and arm blocks, the white fixation cross turned red for 300 ms (warning signal for the movement preparation) and, after a variable delay (750; 1,000; 1,250; and 1,500 ms), turned green (go signal) for 4 s, instructing participants to execute a 4 s sequence of limb movement while keeping central fixation. Specifically, right leg movements consisted in a 2 s initial

phase of foot and joint (ankle, knee, and hip) rightward rotation followed by a leg flexion; it followed an immediate 2 s “back phase” of foot and joint leftward rotation and leg extension to return at the initial resting position (see Figure 1c). Right arm movements consisted in a 2 s initial phase of hand and wrist outward rotation followed by an abduction of the arm diagonally directed to reach the opposite shoulder; it followed an immediate 2 s “back phase” of joint inward rotation and arm adduction returning at its initial resting position at the center of the chest. In both cases, the next trial started after an intertrial interval of 1 s. Four consecutive trials followed each block instruction, and each trial consisted of a single 4 s sequence of leg or arm movements. Before entering the scanner, participants were instructed on movements timing and sequence; in the scanner, they performed a short warm-up phase to familiarize with the task and with the correct movement execution (Figure 1b,c).

The leg movement simulated a step initiation, such as that done when we step on a staircase or when we overcome an obstacle along the way or during climbing, and implied the transport component of the leg, which is fundamental in real-world walking movements. We are aware that leg movement we used does not exactly simulate walking movements and joint rotations of both leg and arm were used as expedients to maximally activate somatomotor cells. Although movements performed by our subjects in the scanner lack the complexity

and the gravitational aspects of real body movements in the environment, it should be noted that technical limits make it difficult to use fMRI for studying real locomotion. An important point is that we used a long-range leg movement (the foot moved along an average distance of 45 cm, range 35–55 cm), which recruits several muscles at the same time and the three main joints of the leg (i.e., ankle, knee, and hip) as well as significant somatosensory feedback, thus sharing some basic elements with locomotion.

## 2.3 | Experimental setup

In the visual motion task, we used a wide field setup similar to that originally described by our group (Pitzalis et al. 2006, 2010; Pitzalis, Bozzacchi, et al., 2013; Pitzalis, Sdoia, et al., 2013; Pitzalis, Sereno, et al., 2013; Strappini et al., 2015, 2017). Shortly, stimuli were projected onto a back-projection screen attached to the back of the head coil, at a distance of about 21 cm from the subjects' eyes and seen in binocular view via an enlarged mirror. Subjects' head was lowered of about 4 cm from isocenter so that even the bottom portion of the screen could be seen. In such conditions, visual stimuli subtended up to 62 by 48° of visual angle. Nevertheless, subjects could comfortably fixate a central point on the screen without blurring.

In the motor task, we used a standard setup where the projection screen was attached to the back of the MR bore, and the average viewing distance was 66.5 cm, subtending 19 by 14° of visual angle. For this task, we used an in-house MRI-compatible setup for leg movements (Figure 1c). Shortly, it consisted in an aluminum track fixed via Velcro straps on a wooden table, which perfectly fitted the scanner table. The aluminum track ended with a foot aluminum support that enabled fluid and controlled right leg movements sliding along the whole track. This setup was central in this study, since it allowed subjects to perform real long-range active leg movements rather than simpler toe/ankle movements as carried out in previous studies (e.g., Heed, Beurze, Toni, Röder, & Medendorp, 2011; Heed, Leoné, Toni, & Medendorp, 2016; Leoné, Heed, Toni, & Medendorp, 2014).

In both tasks, in order to minimize movements during the scans, subjects' head was stabilized with foam padding and with a chin rest mounted inside the head coil. In order to reduce subjects' discomfort, we placed a circularly shaped foam cushion under the inion and additional foams under the participants' back.

## 2.4 | Eye movement recordings

In order to measure fixation stability, we used an infrared ASL eye-tracking system operating at 60 Hz (Applied Science Laboratories, Bedford, MA; Model 504). At the beginning of the experiment, we carried out a nine-point calibration procedure. We calculate the fixation stability (i.e., the position of the right eye in the focal plane) as the *SD* of the eye position averaged along both the horizontal and vertical dimensions (in degrees of visual angle). Since the eye tracker was not compatible with the wide-field setup, fixation was only monitored during the motor scans. We obtained useable data in a subset of subjects (13 out of 18) due to usual reasons (e.g., difficulties maintaining

pupil tracking across the experiment with light-eyed subjects). In addition, we carried out an online visual inspection of gaze position in order to detect unwanted saccades during motor task. The online control was useful also to give participants feedback on excessive blinking or signs of lapses in attention during the runs.

## 2.5 | Image acquisition and preprocessing

We acquired MR images at the Santa Lucia Foundation (Rome, Italy) on a 3T Siemens Allegra MR system (Siemens Medical Systems, Erlangen, Germany) using a standard head coil. Functional T2\*-weighted images were collected using a gradient echo EPI sequence using blood-oxygenation level-dependent (BOLD) imaging (Kwong et al., 1992). Thirty contiguous 3.5 mm slices were acquired in the AC–PC plane with an in-plane resolution of 3 × 3 mm<sup>2</sup> and an interleaved excitation order (0 mm gap), 64 × 64 image matrix, echo time (TE) = 30 ms, flip angle = 70°, repetition time (TR) = 2 s. From the superior convexity, sampling included all the cerebral cortex, excluding only the ventral portion of the cerebellum. In each scan, we discarded the first four volumes from data analysis to achieve a steady state, and the experimental tasks started at the beginning of the fifth volume. Overall, each subject completed two 256-s long visual motion scans, three 526-s long motor scans, and three 256-s long resting-state scans. Structural images were collected using a sagittal magnetization-prepared rapid acquisition gradient echo (MPRAGE) T1-weighted sequence (TR = 2 s, TE = 4.38 ms, flip angle = 8°, 512 × 512 image matrix, 0.5 × 0.5 mm<sup>2</sup> in-plane resolution, 176 contiguous 1 mm thick sagittal slices).

Structural images were analyzed using FreeSurfer 5.1 (<http://surfer.nmr.mgh.harvard.edu/>) to obtain a surface representation of each individual cortical hemisphere in a standard space. We used the “recon-all” fully automated processing pipeline, which, among other steps, performs intensity correction, transformation to Talairach space, normalization, skull-stripping, subcortical and white-matter segmentation, surface tessellation, surface refinement, surface inflation, sulcus-based nonlinear morphing to a cross-subject spherical coordinate system, and cortical parcellation (Dale, Fischl, & Sereno, 1999; Desikan et al., 2006; Fischl, Sereno, & Dale, 1999; Fischl, Sereno, Tootell, & Dale, 1999). We transformed the resulting surface reconstructions to the symmetrical FS-LR space (Van Essen, Glasser, Dierker, Harwell, & Coalson, 2012) using tools in the Connectome Workbench software (<https://www.humanconnectome.org/software/get-connectome-workbench>), resulting in surface meshes with approximately 74K nodes per hemisphere.

Functional images were realigned within and across scans to correct for head movement and coregistered with structural MPRAGE scans using SPM12 (Wellcome Department of Cognitive Neurology, London, UK). Functional data were resampled to the individual cortical surface using ribbon-constrained resampling as implemented in Connectome Workbench (Glasser et al., 2013) and smoothed along the surface with an iterative procedure emulating a Gaussian kernel with a 4 mm full width at half maximum (FWHM) in the visual motion task and with a 6 mm FWHM in the motor task.

## 2.6 | Statistical analysis of the visual motion task

We estimated the hemodynamic responses according to the general linear model (GLM), modeling blocks of coherently moving dot fields as boxcar functions convolved with an idealized representation of the hemodynamic response function as implemented in SPM. We did not explicitly modeled blocks of random motion as GLM regressors that were rather treated as part of the residual variance. We expressed for each area the response to coherent motion as a proportion of the response to random motion. For each participant and region, we computed how much the signal increases in the coherent condition (with respect to the random condition), as a function of the random condition as follows:

$$PSC = \frac{(C-R)}{R} * 100$$

where the PSC represents the percent signal change, *C* represents the BOLD signal to the coherent condition, and *R* represents the BOLD signal to the random condition. We analyzed the visual motion scans on a vertex-by-vertex basis, applying the GLM to the surface-transformed smoothed fMRI images. For each individual hemisphere, we obtained a parametric map of the *t* statistics, representing the activation during coherently moving dots relative to the implicit baseline (randomly moving dots). We corrected the statistical maps for multiple comparisons at the cluster level ( $p < .05$ ) through a topological false discovery rate procedure based on random field theory (Chumbley, Worsley, Flandin, & Friston, 2010), after defining clusters of adjacent vertices surviving at least an uncorrected voxel-level threshold of  $p < .01$ . Individual inspection of hemisphere-specific thresholded maps allowed us to define six regions of interest (ROIs) with a significant response to coherently moving dots relative to random motion: V6+, V3A, IPSmot/VIP, CSv, pCi, and PIC (see Figure 1a). The specific anatomical criteria followed in order to define each ROI are detailed in the Results section. We extracted individual ROIs by isolating single activation peaks and their neighborhood through a watershed segmentation algorithm as applied to surface meshes (Mangan & Whitaker, 1999). A representative time course for each ROI was generated by averaging surface-transformed unsmoothed fMRI images across all vertices within each ROI. Submitting these regional time courses to the GLM, generated regional hemisphere-specific parameter estimates, which were analyzed through a one-way repeated-measures ANOVA with region as factor (computed on a subgroup of 12 subjects in which all six regions could be defined in at least one hemisphere). In this ANOVA, we used Duncan test for conducting post hoc comparisons.

## 2.7 | Statistical analysis of the motor task

We analyzed the motor task firstly at the regional level, since our main aim was to demonstrate whether cortical regions selective for egomotion-compatible visual stimuli (as evidenced from the visual motion task) were also responsive during the motor task. For the analysis of the motor task, we analyzed ROIs only in the left hemisphere

to account for the fact that participants used their right upper and lower limbs: V6+ (18 hemispheres), V3A (12 hemispheres), IPSmot/VIP (13 hemispheres), pCi (11 hemispheres), PIC (18 hemispheres), and CSv (17 hemispheres).

We submitted averaged regional time courses to a GLM modeling blocks of arm and leg movements as boxcar functions convolved with an idealized representation of the hemodynamic response function, and also including six head movement-related parameters as nuisance regressors. We first subjected individual regional parameter estimates representing signal changes in the leg condition to one-sample *t* tests versus zero to reveal regions with significant activations in the leg condition relative to the implicit baseline (fixation). We applied a Bonferroni correction for multiple comparisons ( $p = .05/N = 6$ , number of regions;  $p = .004$ ). To reveal effector-related differences, we conducted an ANOVA with Region (V6+, V3A, IPSmot/VIP, pCi, PIC, and CSv) and experimental condition (leg and arm) as factors. In this ANOVA (computed on a subgroup of 11 subjects in which all six regions could be defined in the left hemisphere), post hoc comparisons were conducted using Duncan's test.

We also conducted a group-level analysis as we were interested in showing the overall extension of motor maps relative to ROI locations and to borders of functional connectivity maps. We compared BOLD signal in each condition (leg and arm movements) to the implicit baseline (fixation) through one-sample *t* tests. Group-level statistical maps were thresholded at  $p < .05$  FDR corrected at the cluster level, after applying a cluster-forming threshold of  $p < .001$  uncorrected at the voxel level.

## 2.8 | Statistical analysis of resting-state fcMRI

To examine the pattern of cortical connections associated with the six (ROIs described above, we implemented a connectivity analysis of the fMRI data recorded at rest using a seed-to-vertex approach in which we estimated a map of covariance from the BOLD signal time course extracted from each ROI. Again, we analyzed only the left hemisphere, since movements were produced through the right arm/leg. fcMRI maps were obtained using vertex-wise multiple regression analysis (see Margulies et al., 2009; Uddin, 2010; Tosoni et al., 2015 for similar data analysis methods). The time course of each ROI was used as a covariate of interest in a GLM applied at each hemispheric vertex. Sources of spurious variance were removed by including extra regressors as nuisance covariates: the global signal time course, estimated as the average BOLD signal within the default SPM within-brain mask, plus several other regressors summarizing voxel time courses in regions where the time series data are unlikely to be modulated by neural activity, to reduce noise due to physiological fluctuations and other sources, such as subject motion (Behzadi, Restom, Liu, & Liu, 2007). More specifically, we included four white matter and four cerebrospinal fluid (CSF) regressors, computed as the first four eigenvariates of a singular value decomposition of the resting state time courses of all voxels within the white matter and CSF, respectively. We also included six head movement regressors to further reduce motion-induced noise. Individual seed time courses were orthogonalized with respect to



nuisance regressors. We finally included constant terms to model overall differences across scans. Before entering the GLM, images were temporally filtered using band-pass filter with cutoff frequencies of 0.1 and 0.01 Hz. The low-pass filter was motivated by fact that the majority of the previous fMRI studies focused on slow (<0.1 Hz) BOLD fluctuations (for a review, see Fox & Raichle, 2007).

We conducted a preliminary connectivity analysis using a seed-to-seed approach in which, for each subject and each pair of ROI, we calculated partial Pearson correlation coefficients between the two corresponding regional BOLD time courses, as an index of the inter-regional temporal coupling between the two regions. We computed partial correlations on “adjusted” time courses, that is, after removing the effect of the sources of spurious variance modeled in the GLM, including the global signal, head movements, and so forth (see above). After transforming correlation coefficients to  $z$  values using the Fisher transform, we used one-sample one-tailed  $t$  tests to assess whether correlation coefficients were significantly higher than zero. We applied a Bonferroni correction for multiple comparisons ( $p = .05/N = 15$ , number of comparisons between six regions;  $p = .003$ ).

To reveal any segregated pattern of cortical connections among egomotion-related areas, at the first level, we generated two subject-specific GLMs, each including three regressors corresponding to three seed regions, grouped according to their functional responses to the motor task: regions not responsive to the motor task (V6+, V3A, and IPSmot/VIP) and regions responsive to the motor task (CSv, pCi, and PIC). At the second level, we generated group fMRI statistical maps for each set of regions using an omnibus  $F$  test where subjects were treated as a random effect. The two resulting maps superimposed and color-coded (red for V6+, V3A, IPSmot/VIP; cyan for CSv, pCi, PIC) in Figure 4, represented brain regions associated at least with one of the regions included in the model. We conducted a corollary analysis aimed at disambiguating the contribution of each seed region to the connectivity maps associated with the two set of regions. To this purpose, we generated separate first-level subject-specific GLMs each including one seed region each. At the second level, we generated group fMRI statistical maps for each seed region using one-tailed one-sample  $t$  test. These maps identify brain regions significantly coupled with each of the seed regions. All group-level fMRI statistical maps were thresholded at  $p < .001$  (uncorrected) and corrected for multiple comparisons at the cluster level using topological FDR ( $p < .05$ ).

We used the Conte69 surface-based atlas (Van Essen et al., 2011) to put our findings in relation to previous parcellations of human cerebral cortex already ported to this atlas, such as those of early visual areas and MT+ based on retinotopic data (Kolster et al., 2010). Note, however, that because these parcellations are typically based on retinotopic or functional data from single subjects or small groups of subjects, descriptions of the overlay between our group functional connectivity maps and areal borders from these parcellations are only illustrative. We compared our results to the motor and somatomotor areas as defined by the classical Brodmann parcellation included in the Conte69 atlas and to other datasets (not included in the atlas) such as and the scene-selective regions parahippocampal place area (PPA, Epstein & Kanwisher, 1998) and retrosplenial complex (RSc,

Epstein, 2008). PPA and RSc were probabilistically defined by averaging individual ROIs from 44 subjects (separate from the participants of the current study) who underwent a localizer fMRI experiment consisting in passive viewing of scenes versus faces pictures (described in Sulpizio et al. (2013)).

## 3 | RESULTS

### 3.1 | Behavior

In the motor task, all participants performed active limb movements as instructed with no exception, and never performed extra limb movements. The gaze position recorded during the fMRI scanning in a subset of subjects (see the Methods section) indicated that the fixation stability throughout the motor task was excellent ( $SD = 1.1^\circ$ ), well in line with standard parameters (e.g., Crossland, Morland, Feely, Von Dem Hagen, & Rubin, 2008; Di Russo, Pitzalis, & Spinelli, 2003; Fischer, Bülthoff, Logothetis, & Bartels, 2012b; Pitzalis, Sereno, et al., 2013). The percentage of unwanted saccades was quite low (3%). Since such saccades were rare and equally distributed across block types, we should not expect this problem to result in any systematic bias, but eventually in a decreased sensitivity in detecting differences between conditions.

### 3.2 | Egomotion-related regions from the visual motion task

To localize areas selectively responsive to coherent optic flow, we compared the BOLD response to coherently versus randomly moving dots. The rationale behind this approach is that we wanted to isolate areas responding to optic flow compatible with egomotion from other visual areas responding to local signal changes (as random motion), which are not compatible with the retinal stimulation evoked by one's own movement into the environment.

Figure 2a shows egomotion-sensitive regions in two representative subjects as resulting from the analysis of the visual motion task, displayed on their inflated left and right hemispheres (lateral and medial views). The results were consistent across participants and allowed to define six distinct cortical regions strongly and bilaterally responsive to egomotion-compatible stimuli. Figure 2b shows the average location of the six regions, projected onto a flattened representation of a standard brain. Table 1 reports MNI coordinates of the centers of mass of individually defined regions, averaged across subjects.

1. The area V6 was identified in all subjects (36/36 hemispheres, 100%) in the parieto-occipital sulcus (POs). Given that the here defined region may also include the more anterior V6Av, which was found to respond to this visual motion task as well (Pitzalis, Sereno, et al., 2013; Tosoni et al., 2015), here we refer to this region as V6 complex (or V6+).
2. Area V3A was consistently found in the ventral portion of the posterior IPS (pIPS). Although here we did not perform retinotopic mapping, we refer to this region as V3A based on our two

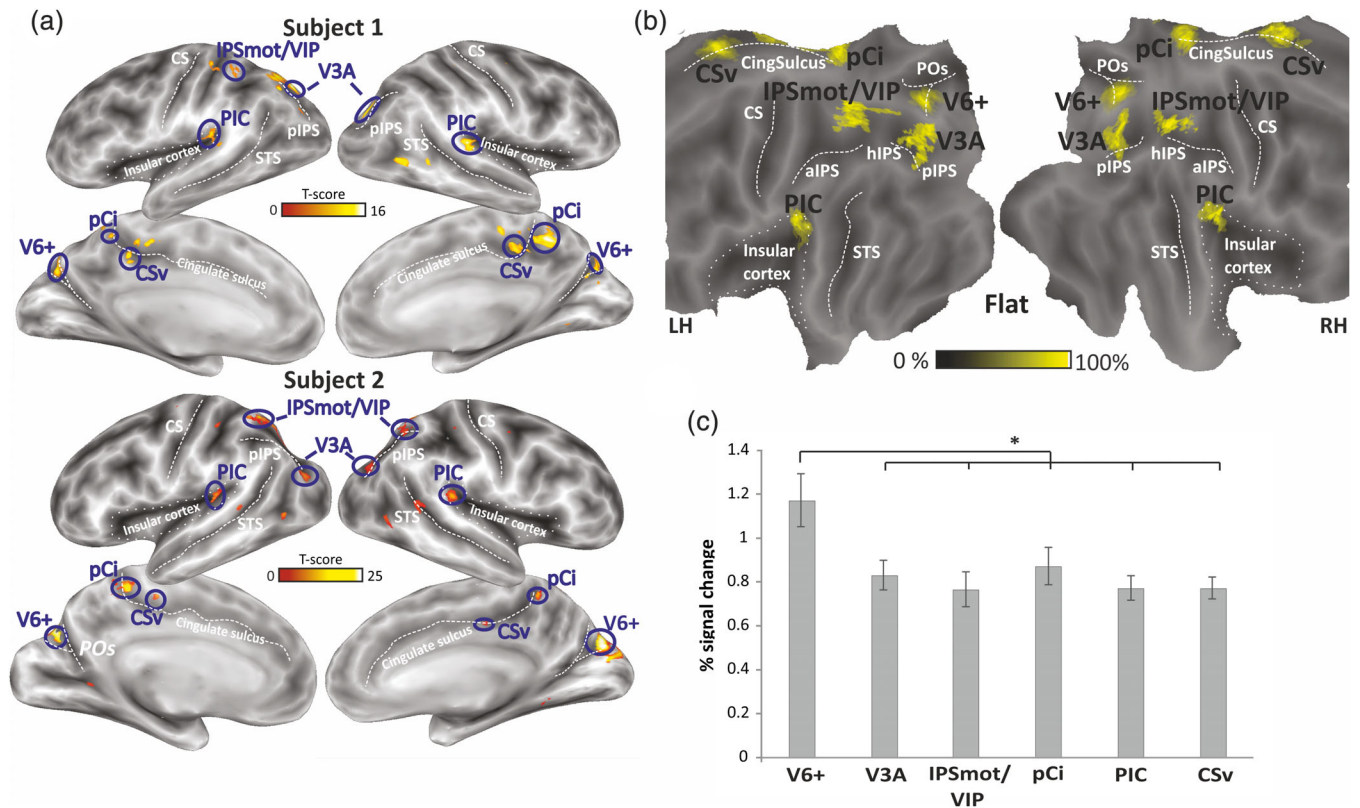


**FIGURE 2** Brain areas selectively responsive to the visual motion task. (a) Examples of individual egomotion-related ROIs (blue circled) defined on the inflated cortical surface reconstruction of the hemispheres of two representative subjects (lateral and medial views) on the basis of the visual motion task. The color scales indicate the statistical significance of individual activations using the FDR corrected  $p$  values at cluster level. (b) Group overlap of the six individually defined bilateral egomotion-related ROIs displayed on the flattened Conte69 surface-based atlas. Each yellow patch represents the weighted average location of individual ROIs. The color bar shows the level of saturation, where solid yellow represents the maximum overlap across 90% of total subjects. (c) Sensitivity of the egomotion-related ROIs to egomotion-compatible stimuli. Column histograms represent the mean percentage of the signal changes  $\pm$  SE of the mean across subjects in each ROI for the coherent motion relative to random motion. \* $p < .0001$ . aIPS, anterior segment of the intraparietal sulcus; CS, central sulcus; CSv, cingulate visual area; hIPS, horizontal segment of the intraparietal sulcus; IPSmot/VIP, intraparietal motion area/ventral intraparietal; pCi, posterior cingulate sulcus area; PIC, posterior insular cortex; pIPS, posterior segment of the intraparietal sulcus; POs, parieto-occipital sulcus; ROI, region of interest; STS, superior temporal sulcus; V6+, V6 complex [Color figure can be viewed at [wileyonlinelibrary.com](http://wileyonlinelibrary.com)]

previous retinotopic studies where we showed that the pIPS activation during the flow field stimulus coincides with the retinotopic area V3A (Pitzalis et al., 2010; Sereno et al., 2001). V3A was identified in 26/36 hemispheres (72%).

3. A parietal region (IPSmot/VIP) was found along the anterior dorsal segment of the IPS (28/36 hemispheres, 78%). This cortical region may correspond to the VIP area described by many authors. However, in human, four different locations have been reported for VIP by Bremmer et al. (2001), Sereno and Huang (2006), Bartels, Zeki, and Logothetis (2008), and Cardin and Smith (2010), respectively (for a review, see Huang, Chen, & Sereno, 2017; Huang & Sereno, 2018). Note that in order to locate the human area VIP, a response to tactile stimulation to the face is necessary in addition to response to coherent visual motion, as originally described by Sereno and Huang (2006) and as reported in a few other papers (e.g., Eger, Pinel, Dehaene, & Kleinschmidt, 2015). Thus, in the absence of bimodal stimulation, the homology question cannot be settled, and for this reason, we previously choose the neutral

name of IPS motion region (IPSmot) to refer to a visual motion region located in the horizontal segment of the IPs (Pitzalis, Sdoia, et al., 2013). Note, however, that the mean coordinates of the region found here (Table 1) and its anatomical position (Figure 2b) are more in line with those of area VIP by Cardin and Smith (2010) than with area IPSmot by Pitzalis, Sdoia, et al. (2013), which is more lateral and slightly posterior than the area found here. For this reason, and because of homology uncertainty, here we refer to this as IPSmot/VIP.

4. The posterior cingulate sulcus area (pCi) was found within the posterior dorsal tip of the cingulate sulcus (27/36 hemispheres, 75%). This region was originally labeled Pc (as precuneus) by Cardin and Smith (2010), but then the same authors referred to it as the precuneus motion area to distinguish it from other parts of the precuneus (Cardin & Smith, 2011; Uesaki & Ashida, 2015; Wada, Sakano, & Ando, 2016). Sereno and coworkers found responses to visuomotor tasks (Filimon, Nelson, Huang, & Sereno, 2009), visual motion stimuli (Huang et al., 2015), and imagined

**TABLE 1** MNI coordinates (mm) of ROIs. Centers of mass of individually defined regions are reported averaged across subjects

Regions	MNI coordinates		
	X	Y	Z
V6+			
LH	-15	-80	27
RH	15	-78	39
V3A			
LH	-23	-85	26
RH	23	-85	24
IPSmot/VIP			
LH	-25	-57	56
RH	29	-52	55
pCi			
LH	-12	-40	54
RH	12	-37	52
PIC			
LH	-40	-36	20
RH	45	-32	24
CSv			
LH	-11	-18	41
RH	12	-18	43

CSv, cingulate visual area; IPSmot/VIP, intraparietal motion area/ventral intraparietal; pCi, posterior cingulate sulcus area; PIC, posterior insular cortex; ROI, region of interest; V6+, V6 complex.

egomotion (Huang & Sereno, 2013) in an extended area of the precuneus labeled either PCu (precuneus) or aPCu (anterior precuneus). However, aPCu was a large area extending from the precuneus into the pCi. Thus, aPCu/PCu included the area Pc originally described by Cardin and Smith (2010) but extended further than area Pc. The region found here strictly corresponds to area Pc by Cardin and Smith (2010). However, to avoid confusion with the other areas of the Pc region and to highlight its correct location within the cingulate sulcus, here we prefer to call it pCi area.

- The PIC was consistently found at the junction between the posterior insula and the posterior parietal cortex (36/36 hemispheres, 100%). This region corresponds to the motion insular area originally defined by Cardin and Smith (2010) and called by them parieto-vestibular insular cortex (PIVC). More recent evidence, however, has shown that along the insula in humans there are two motion regions, named PIVC and PIC (Greenlee et al., 2016). While PIC is a multisensory region, responding to both vestibular and visual stimuli, PIVC (located more anteriorly, in correspondence of the lateral end of the central sulcus) responds to vestibular stimuli only. Thus, previously reported activations in posterior lateral sulcus during self-motion induced by visual motion (e.g., Cardin & Smith, 2010; Huang et al., 2015; Uesaki & Ashida, 2015) might fall within PIC, or at least partially overlap with PIC, rather than PIVC (e.g., Frank et al., 2014; Frank, Sun, Forster, Peter, & Greenlee, 2016; Frank, Wirth, & Greenlee, 2016; Greenlee et al., 2016).

Therefore, as we used here a pure visual stimulation, we refer to this region as area PIC.

- The CSv area was located in the depth of the posterior part of the cingulate sulcus, anterior to the posterior ascending portion of the cingulate sulcus (35/36 hemispheres, 97%). This location well corresponds to the original definition of human CSv provided by Wall and Smith (2008).

Moreover, three additional activations were sometimes found in: (a) MT+, in between the inferior and the middle temporal sulcus (69%); (b) p2v, at the dorsal portion of the postcentral sulcus (64%); and (c) STS, in the posterior segment of the superior temporal sulcus (47%). Note that in the two representative subjects shown in Figure 2a, these additional regions are variably present. Given the weak consistency across subjects (lower than 70%), we did not include them in the set of the selected egomotion-related ROIs for further analyses.

To explore the differential sensitivity of the resulting regions to egomotion-compatible stimuli, we computed the percent signal change for egomotion-compatible versus random motion (Figure 2c). A one-way repeated-measures ANOVA with region as factor revealed a significant main effect of region ( $F_{(5,55)} = 7.19, p < .0001$ ). Post hoc tests indicated that the BOLD response was significantly higher in V6+ than in all other regions, which did not differ against each other.

### 3.3 | Functional profiles during the motor task and seed-to-seed connectivity of egomotion-related regions

We studied the functional response profile of the six egomotion-related areas during the motor task to explore their sensitivity to active leg movements. The mean percent signal change observed in each of these regions for the two motor conditions (leg and arm) is plotted in the column histograms of Figure 3a.

In order to reveal regions with a significant response to leg movements, we used one-sample *t* tests versus zero in each region. Results revealed that three areas pCi, PIC, and CSv responded to leg movements (pCi,  $t_{10} = 3.33, p = .007$ ; PIC,  $t_{17} = 4.94, p = .0001$ ; CSv,  $t_{16} = 3.26, p = .004$ ; *p* value Bonferroni corrected), while the other three, V6+, V3A, and IPSmot/VIP, did not (V6+,  $t_{17} = -1.03, p = .31$ ; V3A,  $t_{11} = -0.91, p = .37$ ; IPSmot/VIP,  $t_{12} = 1.01, p = .33$ ).

To reveal any significant effector-related differences, beta values underwent an ANOVA with region (V6+, V3A, IPSmot/VIP, pCi, PIC, CSv) and condition (leg and arm) as factors. Duncan's post hoc tests on the significant region by condition interaction ( $F_{(5,50)} = 11.61, p < .001$ ) confirmed that pCi, PIC, and CSv were more activated by leg than arm movements (all regions:  $p < .001$ ), while V6+ and V3A showed a greater signal decrease in the arm than leg condition (both regions:  $p < .001$ ). IPSmot/VIP did not show any significant difference between the two conditions ( $p = .11$ ). Notably, in the leg condition, pCi and PIC responded significantly more than V6+, V3A, and IPSmot/VIP (all regions:  $p < .001$ ), while CSv more than V6+ and V3A ( $p < .05$ ).



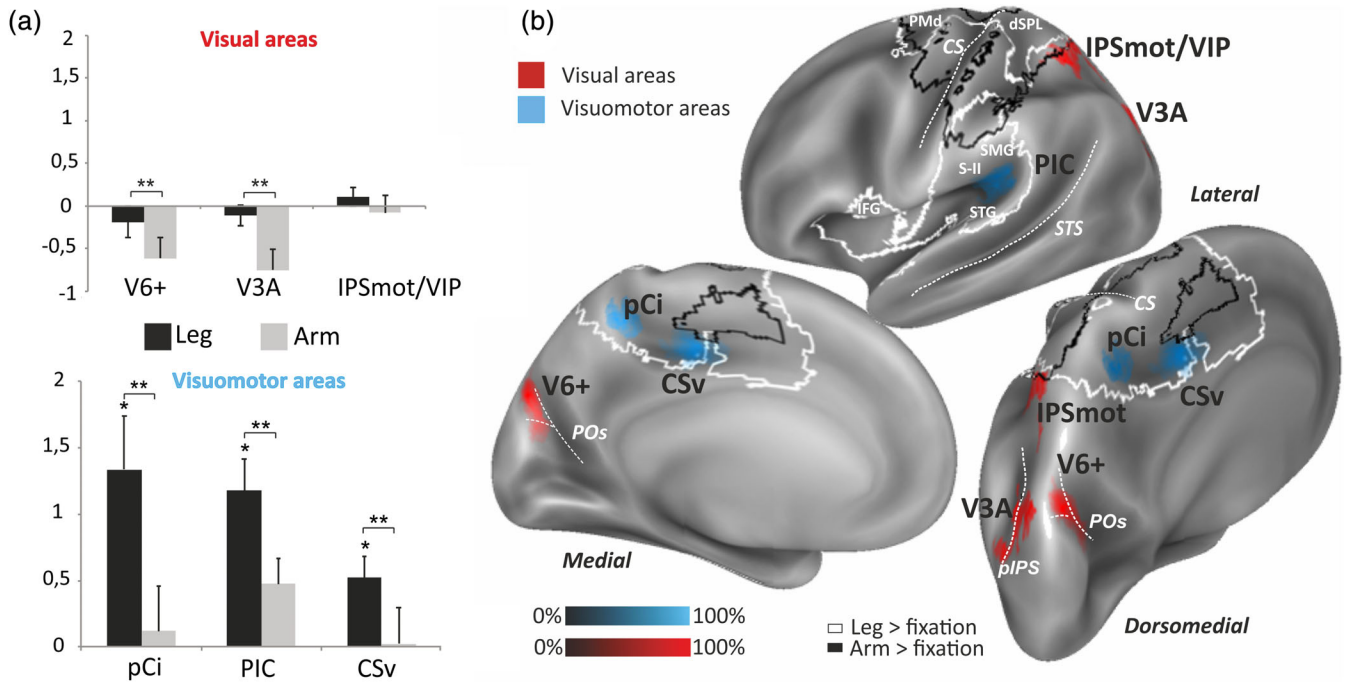


**FIGURE 3** Regions sensitivity to active limb movements. (a) Column histograms plot the mean percentage of signal changes  $\pm$  SE of the mean across subjects in each ROI for leg and arm conditions relative to the fixation baseline. Asterisks mark significant effect of condition. \* $p < .01$ . \*\* $p < .001$  (Bonferroni corrected). Other labels are as in Figure 2. (b) Overlap of the six individually defined egomotion-related ROIs rendered on the inflated representation of the left hemisphere of Conte69 surface-based atlas. ROIs colors indicate in red visual areas not responding to limb movements (V6+, V3A, and IPSmot/VIP) and in cyan visuomotor areas responding to leg movements (pCi, PIC, and CSv). The level of overlap across subjects is indicated by the gradient saturation of the color bar as in Figure 2. The white and black outlines indicate the cortical network activated by the leg > fixation and arm > fixation contrasts, respectively. CSv, cingulate visual area; IPSmot/VIP, intraparietal motion area/ventral intraparietal; pCi, posterior cingulate sulcus area; PIC, posterior insular cortex; ROI, region of interest; V6+, V6 complex [Color figure can be viewed at [wileyonlinelibrary.com](http://wileyonlinelibrary.com)]

We performed an analysis of functional connectivity using seed-to-seed partial correlations for each pair of ROIs (Table 2). This analysis confirmed that regions responding (pCi, PIC, and CSv) or not responding (V6+, V3A, and IPSmot/VIP) to leg reflect two distinct (quite segregated) functional networks. We found indeed significant couplings exceeding the Bonferroni-corrected significance threshold ( $p < .003$ ) between V3A and both V6+ ( $t_{11} = 4.06$ ;  $p < .01$ ) and IPSmot/VIP

( $t_9 = 6.67$ ;  $p < .0001$ ) and between CSv and both pCi ( $t_9 = 7.37$ ;  $p < .0001$ ) and PIC ( $t_{16} = 5.22$ ;  $p < .0001$ ). Beyond these correlations, we also found significant couplings between visual and visuomotor areas, that is, between CSv and IPSmot/VIP ( $t_{12} = 5.07$ ;  $p < .001$ ) and between PIC and V3A ( $t_{11} = 6.80$ ;  $p < .0001$ ), indicating a partial crosstalk between these two set of areas.

**TABLE 2** Seed-to-seed partial correlations. Significant Pearson correlations coefficients (one-tailed t test against zero) are marked with asterisks

	V6+	V3A	IPSmot/VIP	pCi	PIC	CSv
V6+	1					
V3A	.243*	1				
IPSmot	.101	.304***	1			
pCi	.177	.003	.082	1		
PIC	.097	.206***	.126	.109	1	
CSv	.123	.065	.15**	.352***	.221***	1

CSv, cingulate visual area; IPSmot/VIP, intraparietal motion area/ventral intraparietal; pCi, posterior cingulate sulcus area; PIC, posterior insular cortex; ROI, region of interest; V6+, V6 complex.

\* $p < .01$ . \*\* $p < .001$ . \*\*\* $p < .0001$ . Bonferroni corrected.

Beyond the regional approach, we conducted also a whole-brain analysis to show the relation between brain regions involved in leg and arm movements and the six egomotion-related regions. Figure 3b shows leg > fix (white outline) and arm > fix (black outline) contrasts. The cortical network for leg movements included a wide network including not only the medial primary motor and somatosensory cortices (M-I and S-I, corresponding to the cortical territory where lower limbs are represented) but also parietal (dSPL, SMG), frontal (PMd, SMA, IFG), and temporo-insular (STG, S-II) regions. The cortical network for arm movements included a distributed network of areas encompassing the lateral portion of M-I and S-I (corresponding to the cortical territory where upper limbs are represented), the PMd, the dSPL and ventrally into the SMG. In the medial surface of the hemisphere, we also found activation in the anterior CMA. Even though literature focusing on lower limb is rare, our results are in line with previous studies showing parieto-frontal activations during active/passive execution of simple leg

or foot movements (Christensen et al., 2007; Cunningham, Machado, Yue, Carey, & Plow, 2013; Dalla Volta et al., 2015; Lorey et al., 2013; Luft et al., 2002; Rocca & Filippi, 2010; Sahyoun, Floyer-Lea, Johansen-Berg, & Matthews, 2004). In comparison to previous studies on locomotion testing bipedal movements (e.g., Dalla Volta et al., 2015), we found an even more extended network of activations involving also insular cortex and parietal and cingulate midline areas. This could be explained by the long-range movement required in our study. Fully rotating, flexing, and extending the leg requires more computations, recruits a larger number of muscles, involves several joints, lasts longer and involves more somatosensory feedback than a simple ankle rotation/flexion (e.g., Cunningham et al., 2013). In the motor task, we did not use visual stimuli deliberately and subjects did not receive visual feedbacks about their leg positions, as we were interested in isolating effects related exclusively to motor stimulation. This might be the reason why we did not observe ventral activations in the inferior parietal lobe or in the parieto-occipital site, as found in previous studies (Christensen et al., 2007; Cunningham et al., 2013; Sahyoun et al., 2004) when visual feedback about foot movements was provided.

Overall, as expected from the regional analyses, the cortical network for leg movements included the three visuomotor regions (pCi, CSv, PIC) but not the three visual regions (V3A, V6+, IPSmot/VIP). None of the six regions was part of the cortical network for arm movements, although note that area IPSmot/VIP was right at the border of the black outline, with a few nodes falling within the outline. Based on these results, we refer to the set of egomotion-related areas responding to leg movements (pCi, PIC, and CSv) as visuomotor areas (cyan in Figure 3b), and to the set of areas not responding to limb movements (V6+, V3A, and IPSmot/VIP) as visual areas (red in Figure 3b).

### 3.4 | Resting-state connectivity of egomotion-related regions

After observing a functional segregation within these two sets of motion regions, we explored the pattern of cortical functional connections of the identified areas to determine whether they belong to segregated or overlapping cortical networks. According to our hypothesis, an egomotion area playing a role in the motor control during locomotion should show functional connectivity with the medial part of somatosensory and motor areas (where foot and leg are represented) and with motor and premotor cortices, differently from regions playing a visual role in egomotion perception. We are aware that functional connectivity is difficult to interpret because it is an indirect, relative measure of neural activity fluctuations. As a result, the relation between fMRI connectivity data and cortical projections by tracer injections in macaque is often not straightforward (Buckner, Krienen, & Yeo, 2013; Smith, Beer, et al., 2017) and physiological data from other sources (e.g., invasive intracerebral recordings, Avanzini et al., 2016) might assist to confirm and interpret the cfMRI finding. However, although caution is needed in the interpretation of the results, intrinsic functional

connectivity provides a powerful noninvasive tool to provide insight into human brain organization.

Functional connectivity maps associated with each of the six seed regions are shown in Figure 4a,c. Furthermore, we generated two distinct fcMRI maps reflecting the connectivity pattern associated with the visual areas (V6+, V3A, IPSmot/VIP) and to the visuomotor areas (pCi, PIC, CSv), respectively. Figure 4b shows the result of the comparison between fcMRI maps of the visual (red patches) and visuomotor (cyan patches) areas. To illustrate the relation between our findings and the location of specific visual and motor areas, we overlaid the resulting connectivity maps onto the Conte69 brain atlas (Van Essen et al., 2011) along with visual, motor, and somatosensory areas as originally included in the Brodmann parcellation and along with the scene-selective regions PPA and RSc as probabilistically defined in a separate set of participants from our database (see the Methods section for details).

Figure 4 suggests that visual and visuomotor areas belong to segregated connectivity networks. Specifically, the visual areas (Figure 4a,b) were preferentially connected with the dorsal occipital cortex, including areas V3A and V7, and small parts of V3 and V3B. The functional connectivity map also included the dorsal POs (anterior and posterior banks) up to the junction between the ventral portion of the POs and the calcarine fissure. This cortical territory contains the RSc region, involved in spatial navigation in humans (Byrne, Becker, & Burgess, 2007). The functional connectivity map extended into PPA and for two visual areas (V6+ and V3A) included also the representation of the upper and lower peripheral visual fields in the ventral and dorsal portions of V1 and V2, respectively. Laterally, functional connections of visual areas reached the dorsal portion of the IPS, extending anteriorly up to the postcentral sulcus (i.e., the anterior portion of the IPS). Ventrally, in the lateral occipital-temporal cortex, visual areas were functionally connected with the visual latero-occipital complex LOR (mainly LO2), the motion sensitive areas V4t, FST, MST, and only a portion of MT. Frontally, functional connections of visual areas were observed with a small portion of the orbitofrontal cortex, overlapping BAs 46 and 11, and with a portion of BA 6, at the junction between the dorsal portion of the precentral sulcus and the superior frontal sulcus, where hand reaching-related responses have been found (Tosoni, Galati, Romani, & Corbetta, 2008). As evident from Figure 4a, connections with this portion of premotor area is mainly explained by the fcMRI map associated with IPSmot/VIP area.

The functional connectivity map associated with visuomotor areas (Figure 4b,c) extended more anteriorly than those associated with visual areas: the two maps were mostly segregated with only minor regions of overlapping. Specifically, visuomotor areas were functionally connected medially with the paracentral lobule, in correspondence with the primary sensory-motor regions, known to be responding to tactile stimulation and to executed or imagined movements of the lower limbs (Akselrod et al., 2017; Dalla Volta et al., 2015; Di Russo et al., 2006; Huang, Chen, Tran, Holstein, & Sereno, 2012; Kapreli et al., 2008). The functional connectivity map partially extended into the medial extension of the BA 6, overlapping the supplementary motor area (SMA) but not the most anterior pre-SMA in accordance

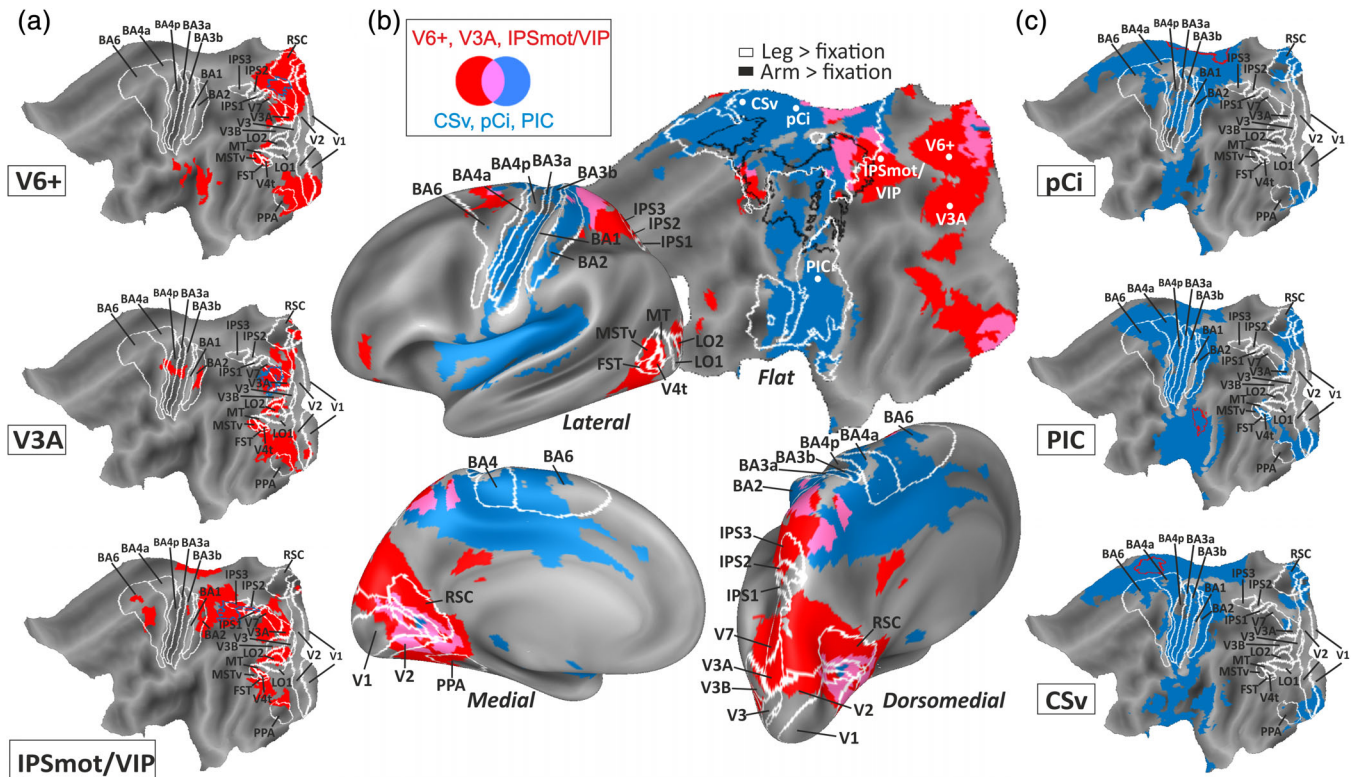


**FIGURE 4** Functional connectivity maps of egomotion-related ROIs. Functional connectivity maps associated with the three seed visual regions (a, blue color outlined over red patches) and the three seed visuomotor regions (b, red color-outlined over blue patches) superimposed over flattened representation of the left hemisphere of Conte69 surface-based atlas. The borders of previously identified areas (Brodmann, 1909/1925; Kolster et al., 2010; Sulpiuzio, Committeri, Lambrey, Berthoz, & Galati, 2013; Van Essen, Glasser, Dierker, Harwell, & Coalson, 2011) are outlined in white (see the Methods section for details). (c) Overlap of two functional connectivity maps, one associated with the group of ROIs not responding to leg movements (visual areas, red patches) and the other associated with the group of ROIs responding to leg movements (visuomotor areas, cyan patches). Light purple patches represent overlapping pattern between the two fcMRI maps and reflect shared connections. Connectivity maps are superimposed over the flattened and inflated (lateral, dorsomedial, and medial views) representation of the left hemisphere of Conte69 surface-based atlas. The borders of previously identified areas (Brodmann, 1909/1925; Kolster et al., 2010; Sulpiuzio et al., 2013; Van Essen et al., 2011) are outlined in white (see the Methods section for details). In the flat map, the white and black outlines indicate the cortical network activated by the leg > fixation and arm > fixation contrasts, respectively. The centers of mass of V6+, V3A, IPSmot/VIP, pCi, PIC, and CSv are marked by a white spot. CSv, cingulate visual area; IPSmot/VIP, intraparietal motion area/ventral intraparietal; pCi, posterior cingulate sulcus area; PIC, posterior insular cortex; ROI, region of interest; V6+, V6 complex [Color figure can be viewed at [wileyonlinelibrary.com](http://wileyonlinelibrary.com)]

with other studies (Picard & Strick, 1996; Zhang & Li, 2012). More ventrally, visuomotor areas were functionally connected with the posterior and middle portions of the cingulate sulcus, where motor responses organized in a somatotopic fashion have been recorded (Amiez & Petrides, 2014). Laterally, the fcMRI map included vestibular and proprioceptive regions, the insular cortex, and the secondary somatosensory cortex (S2), described as roughly somatotopically organized (Eickhoff, Amunts, Mohlberg, & Zilles, 2006; Ruben et al., 2001; Smith, Beer, et al., 2017). Most importantly, visuomotor areas pCi, PIC, and CSv were strongly connected with both the somatosensory (S1; BA 1, 2, 3a, 3b) and the primary motor cortex (M1; BA 4a, 4p).

Although the functional connectivity maps associated with the two sets of egomotion areas were quite segregated, there were also a few overlapping regions. Specifically, shared connections were found in a small portion of visual areas V1 and V2 corresponding to their peripheral representation and in the neighboring territory, likely

including the retinotopically organized prostriate area (Mikellidou et al., 2017). Additionally, we found common functional connections in the dorsal portion of the SPL (near to the postcentral sulcus). This SPL region overlaps with the multisensory parietal face and body areas in humans (Huang et al., 2012). Its ventral part (in the lateral view of Figure 4b) likely corresponds to human VIP (Sereno & Huang, 2006), while its dorsal/medial part contains a lower limb representation that overlaps with lower visual field representation. Interestingly, this parietal homunculus (responding to visual and tactile stimuli) is connected to both visual and visuomotor regions in support of the hypothesis that it integrates multisensory information. Notably, common functional connections extend in the very medial portion of SPL, extending medially just posterior to the cingulate sulcus. In this cortical territory, a multisensory area PEC has been identified in the monkey brain (Pandya & Seltzer, 1982) which uses both visual and somatomotor information, in particular from lower limbs, likely aimed at controlling and guiding body

movements during locomotion (Bakola, Gamberini, Passarelli, Fattori, & Galletti, 2010; Breveglieri, Galletti, Gamberini, Passarelli, & Fattori, 2006; Breveglieri, Galletti, Monaco, & Fattori, 2008; Gamberini et al., 2018).

The flat map of Figure 4b shows the relation between the functional connectivity maps and the cortical network for leg (white outline) and arm (black outline) movements. Note that the functional connectivity maps associated with the three regions responding to leg movements (pCi, CSv, PIC; cyan patches) overlap mainly with the white outline that is with areas responding to leg movements in frontal, parietal, insular, and cingulate cortices. In contrast, the overlap between the two outlines and the functional connectivity maps associated with V6+, V3A, and IPSmot/VIP (red patches) is minimal (if any). This offers strong evidences to our hypothesis that pCi, CSv, and PIC, but not V6+, V3A, and IPSmot/VIP, are part of a wider network specialized in whole-body movements, and particularly in coordinating movements of the lower limbs. Moreover, the good match between functional connectivity maps and task-related activation, indirectly, supports the use of fcMRI data for making reliable interpretation about the functional role of cortical brain regions.

## 4 | DISCUSSION

In the present study, we tested whether the human visual motion areas involved in processing optic flow signals simulating self-motion are also activated by active lower limb movements, and hence are likely involved in guiding human locomotion. In addition, we showed the overall extent of actual sensorimotor activation during limb movements relative to ROIs locations and along with the functional connectivity maps. Since area IPSmot/VIP found here corresponds to area VIP by Cardin and Smith (2010), for the sake of clarity in the discussion, we call this region IPSmot/VIP when we refer to the fMRI literature using visual motion stimuli to define it. In contrast, we call this region VIP when we refer to the macaque literature and to the fMRI literature using bimodal stimulation to define it.

### 4.1 | Areas pCi, CSv, and PIC respond to leg movements and have motor connections

We found fMRI activations for the motor task in three visually mapped areas: pCi, PIC, and CSv. Regional and group-level analysis agreed in showing that these three regions were activated during leg but not arm movements, suggesting a selective role in the motor control of lower limbs movements.

It is known that the cingulate cortex (where pCi and CSv are located) participates in the cortical network monitoring head and body movements in space, as well as in visuospatial attention (Corbetta, Miezin, Shulman, & Petersen, 1993; Gitelman et al., 1999; Kim et al., 1999; Mesulam, 1999). CSv and pCi are both sensitive to wide-field egomotion-compatible stimuli (Antal, Baudewig, Paulus, & Dechent, 2008; Cardin & Smith, 2010; Field, Inman, & Li, 2015; Fischer et al., 2012b; Pitzalis, Sdoia, et al., 2013; Wada et al., 2016) and CSv also

receives vestibular input (e.g., Greenlee et al., 2016; Smith et al., 2012; Smith, Beer, et al., 2017).

Like CSv and pCi, also PIC, located in the caudalmost portion of the sylvian fissure, shows vestibular responses (Fasold et al., 2002; Frank, Sun, et al., 2016; Frank, Wirth, et al., 2016). Area PIC is a motion region responding to visual and vestibular motion. It is considered the “hub” of vestibular information (Frank et al., 2014; Frank, Sun, et al., 2016; Frank, Wirth, et al., 2016) and it presumably participates with the secondary somatosensory area (S2, Eickhoff, Weiss, Amunts, Fink, & Zilles, 2005; Eickhoff et al., 2006) to the integration of motion information from visual and vestibular senses for the perception of self-motion (Frank, Sun, et al., 2016; Frank, Wirth, et al., 2016). A recent study by Huang et al. (2015) found that the right PIC (there called PIVC) responds to active dodges suggesting that it plays an active role in sensing and guiding translational egomotion.

The pattern of functional cortical connections of these three areas (Figure 4b,c) appears consistent with a role in the motor control of leg movements. pCi, PIC, and CSv shared a plurality of connections extending to medial somatosensory and motor cortices. Several studies showed that sensory and motor inputs from legs and feet are mostly represented in medial portions of the cortex (Zlatkina, Amiez, & Petrides, 2016; Akselrod et al., 2017; Tal, Geva, & Amedi, 2017; Chen, Kreuz-Delgado, Sereno, & Huang, 2017), which include primary somatosensory and motor cortices. Movements of leg elicited selective activations also in the cingulate motor area (CMA), along the cingulate sulcus (Amiez & Petrides, 2014) and in the most caudal portion of the supplementary motor cortex, in the cingulate gyrus (Cauda, Geminiani, D'agata, Duca, & Sacco, 2011; Fried et al., 1991). Despite their vicinity, it has been demonstrated that CSv did not overlap with regions of CMA, selectively responsive to hand-guided joystick movements (Field et al., 2015). Notice that the connections between CSv and sensory and motor regions described by present data are well in agreement with a recent fMRI study exploring the CSv connectivity pattern with a combination of resting-state and diffusion-based tractography imaging analyses (Smith, Beer, et al., 2017).

In addition to somatomotor connections, the present results show that pCi, PIC, and CSv are also functionally connected with peripheral early visual areas V1–V2 and with a large cortical territory, including the insular cortex and the posterior part of the perisylvian cortex, which likely includes the PIVC known to be the potential hub of the cortical vestibular network (Frank, Sun, et al., 2016; Frank, Wirth, et al., 2016).

Furthermore, we have also found that pCi, PIC, and CSv share common functional connections with visual areas in the ventral part of the calcarine scissure, where it has been recently identified the human prostriate area (Mikellidou et al., 2017), a retinotopic region representing the far periphery, responsive to fast motion. It is likely that peripheral input in those areas reflect the visual processing of fast object movements (Mikellidou et al., 2017), when they are approaching us, or we are moving towards them, for guiding coordinated responses. Areas of the dorsal visual stream as V6, VIP, and V3A might use visual motion cues to inform sensory and motor region and to guide the body in acting upon those objects (Galletti & Fattori, 2003, 2018). Crucially, it has been demonstrated using PET that visual input from the dorsal



visual stream reaches the dorsal pCi cortex, where pCi and CSv are located, as well as supplementary/presupplementary motor cortices via middle cingulate areas, directly bridging visual and motor areas (Vogt, Vogt, & Laureys, 2006). Finally, shared connections between visuomotor and visual areas are found in a restricted dorsomedial portion of the SPL (Figure 4), extending medially just posterior to the cingulate sulcus where multisensory regions were found in both humans (e.g., VIP and PBA; Sereno & Huang, 2006; Huang et al., 2012) and macaque monkeys (e.g., PFC; Bakola et al., 2010; Breveglieri et al., 2006, 2008; Gamberini et al., 2018).

Taken together, the above-described fMRI and fcMRI patterns suggest that pCi, PIC, and CSv provide sensory information to the motor system for use in guiding whole-body motion. Specifically, an important function of pCi and CSv may be to feed visual and possibly vestibular information about self-motion into a medial motor system concerned with control of locomotion. Of course, it is possible that these regions are involved in all tasks where the visual information is used to guide the legs, like not only locomotion but also, for instance, kicking a ball under visual guidance while standing still. However, since optic flow is one of the most informative dynamic visual cues about our motion in the environment, the combined response of these areas to optic flow and leg movements strengthens the hypothesis that these regions are mainly involved in all classes of actions occurring during egomotion, like walking, running, or stepping on a staircase. A similar interpretation, limited to area CSv and exclusively based on its pattern of cortical connection, has been previously suggested by Smith, Beer, et al. (2017). Here, we substantiated this hypothesis by showing that CSv, together with pCi and PIC, responds to a pure motor task involving leg movements.

#### 4.2 | Areas V6+, V3A, and IPSmot/VIP do not respond to leg movements and do not have motor connections

Unlike the cingulate and sylvian areas, V6+, V3A, and IPSmot/VIP responded to the visual motion task but not to the leg movement execution. The BOLD activity during arm movements was not significant in area IPSmot/VIP, and even inhibited in areas V6+ and V3A. In humans, these three egomotion-related regions have properties that constitute important prerequisites for a visual analysis of the retinal signals due to self-motion. First, V6+, V3A, and VIP are retinotopically organized and respond to the entire contralateral hemifield (Pitzalis et al., 2006; Tootell et al., 1997; Sereno & Huang, 2006). Second, these three areas are well activated by optic flow (Cardin, Sherrington, Hemsworth, & Smith, 2012; Morrone et al., 2000; Pitzalis et al., 2010; Pitzalis, Strappini, De Gasperis, Bultrini, & Di Russo, 2012; Smith, Wall, Williams, & Singh, 2006; Wall & Smith, 2008), which constitutes a rich source of visual cues that can facilitate navigation through the external environment. Third, V3A and IPSmot/VIP respond to changes of heading directions (Furlan et al., 2014; Huang et al., 2012), which is another important visual cue that contributes to the perception of self-motion. Fourth, V6+ and IPSmot/VIP are specialized in distinguishing among different types of self-movement, showing a strong response to

translational egomotion (Pitzalis, Sdoia, et al., 2013) that allows to extract information about the relative distance of objects, useful to act on them, or to avoid them (see also Cardin et al., 2012). Areas V3A and V6+ are likely involved in flow parsing, contributing to perceptual stability during pursuit eye movements (Fischer et al., 2012a; Galletti et al., 1990; Galletti & Fattori, 2003, 2018). Finally, area IPSmot/VIP (but not V6+) shows vestibular responses and appears to integrate visual and vestibular cues to direct self-motion (e.g., Billington & Smith, 2015; Greenlee et al., 2016; Smith et al., 2012; Smith, Greenlee, et al., 2017; Smith, Beer, et al., 2017). Overall, some of these regions could be involved in the extraction of optic flow for the computation of heading direction (V3A, IPSmot/VIP), others for obstacle avoidance (V6+, IPSmot/VIP), and/or for visual/vestibular cue integration (IPSmot/VIP).

The pattern of functional cortical connections of V6+, V3A, and IPSmot/VIP is in support of their visual role in the egomotion signal processing. Their connectivity pattern extended more posteriorly than that of the visuomotor areas (Figure 4), including visual and motion-selective regions that are distributed in medial parieto-occipital and lateral occipitotemporal cortex. In support of the hypothesized visual role in the egomotion perception, a recent study by Schindler and Bartels (2016) found increased functional connections between early visual areas V1 and V2 and high-level visual regions V6+ and V3A during the observation of coherent motion. These connections would mediate the activity of V6+ and V3A in sending back to early visual areas sensory predictions about heading direction extracted from coherent motion. In addition, here, we found that the three visual areas (V6+, V3A, and IPSmot/VIP) are functionally connected with PPA (Figure 4a,b), which is involved in spatial navigation (Epstein, 2008; Sulpizio et al., 2013; Sulpizio, Boccia, Guariglia, & Galati, 2016; Sulpizio, Committeri, & Galati, 2014) and responds to visual real motion in a world-centered reference frame (Korkmaz Hacialihafiz & Bartels, 2015), providing input to stable perception. In Tosoni et al. (2015), we have already observed the presence of functional connections between PPA and V6+. Here, we show that the crosstalk between the dorsal and the ventral stream also extends to other visual-motion areas, such as V3A and IPSmot/VIP. Notably, Sherrill et al. (2015) observed that the functional connectivity between egomotion-related regions, V6+ and V3A, and navigationally relevant regions, RSc and PPA, increased during a first-person navigational task. The authors proposed that this functional link might reflect the ability to update representations of spatial positions based on self-motion cues inferred from first-person navigation perspective. Finally, as shown in Figure 4a, IPSmot/VIP showed functional connections spreading more anteriorly than V6+ and V3A, in the SPL, reflecting its multisensory role in integrating visual, tactile, and vestibular stimuli (Bremmer, Duhamel, Ben Hamed, & Graf, 2002; Chen, DeAngelis, & Angelaki, 2011b; Colby, Duhamel, & Goldberg, 1993; Duhamel et al., 1998). Recently Huang et al. (2017) found that visual and tactile maps in human VIP were centered on the face. They suggested that this area likely plays a role in detecting objects intruding into one's personal space; and when they are perceived as potential threats, VIP was suggested to participate in promptly initiating and guiding defensive movements (Graziano & Cooke, 2006). In line with these

interpretations, here, we found that area IPSmot/VIP is functionally connected with regions in the frontal cortex, partially overlapping the pointing-selective frontal reach region (Tosoni et al., 2008) and the saccade-selective frontal eye fields (Paus, 1996). These connections might mediate avoidance movements in response to looming objects approaching the face (Graziano & Cooke, 2006).

### 4.3 | Flow fields: A functional localizer of six egomotion-related areas

A final note goes to the use of the flow field stimulus as a functional localizer for egomotion-related visual areas. This stimulus was originally found to be able to activate human areas V3A, V6, and V6Av (or V6 complex, V6+) in our previous retinotopic brain mapping studies (Pitzalis et al., 2010; Pitzalis, Sereno, et al., 2013; Sereno et al., 2001) using a posterior coverage of the brain which included only occipital regions and the posterior part of temporal and parietal cortices. Additional egomotion-selective areas (originally named VIP, CSv, Pci, and PIVC) were found by Smith and coworkers using a visual motion stimulus constituted by an array of moving dots arranged in an egomotion-consistent or egomotion-inconsistent pattern (Cardin & Smith, 2010, 2011; Wall & Smith, 2008). In the current study, covering the entire cerebral cortex, we showed that at single-subject level, the flow field stimulus is able to detect four egomotion-related regions (IPSmot/VIP, pCi, PIC, and CSv) in addition to the original V3A and V6+. Our results are in agreement with recent studies that have demonstrated the activation of V6+, IPSmot/VIP, CSv, pCi, and PIC in response to visual motion, including different types of optic flow stimulation (for a review, see Greenlee et al., 2016). In addition, we found that V6+ prefers more than other regions the coherent visual motion generated by the flow field stimulus, confirming the efficacy of flow fields as a functional localizer for this area. Although all six areas were reliably mapped in most subjects, some of these areas (namely, V6+, PIC, and CSv) have been identified with the greatest consistency across subjects. Overall, these findings strongly suggest that the two optic flow stimulations, flow fields (Pitzalis et al., 2010; Pitzalis, Bozzacchi, et al., 2013; Pitzalis, Fattori, & Galletti, 2013; Pitzalis, Sdoia, et al., 2013; Pitzalis, Sereno, et al., 2013), and egomotion-compatible/incompatible stimuli (Cardin & Smith, 2010; Wall & Smith, 2008), are comparable according to their sensitivity to map a network of egomotion-related areas.

## 5 | CONCLUSIONS

As originally reported by Cardin and Smith (2010), a visual-only stimulation simulating the visual changes occurring on the retina during the observer's motion is able to activate several visual and vestibular regions. The main goal of the present study was to verify whether egomotion-related visual areas either contribute exclusively to the visual analysis of egomotion-like signals or are also activated by lower limb movements, that in nature accompany egomotion. We believe that an egomotion area playing a motor role in human locomotion should respond during lower limb movements and not only during the

passive viewing of optic flow. We showed that pCi, PIC, and CSv respond to both visual and motor tasks and are functionally connected with anterior and sensorimotor regions (where leg and foot are represented). Notably, pCi, PIC, and CSv were even effector-selective, responding to leg but not to arm movements. This selectivity reinforces the concept that their function is strictly related to the lower limbs and not to a broader representation of action (Filimon, Nelson, Hagler, & Sereno, 2007) or to a general attentional effect (i.e., a greater deployment of spatial attention during the movement execution than during fixation). We suggest that pCi, PIC, and CSv perform the visual analysis of egomotion-like signals and process motor signals from the lower limbs to provide sensory-motor information to the motor system with the aim of guiding locomotion.

Although caution is needed in the presentation of the functional connectivity data (Buckner et al., 2013; Smith, Beer, et al., 2017), the demonstration of functional heterogeneity as well as of differences in functional connectivity between visual and visuomotor areas suggests that they likely perform different functions within a network aimed at subserving sensory-motor integration during our movement in the external environment. The most posterior regions V6+, V3A, and IPSmot/VIP seem mainly involved in the visual analysis of the egomotion retinal components (as the flow parsing mechanism), necessary to orchestrate eye, arm, and body movements while navigating in a complex and dynamic environment. In contrast, the most anterior regions pCi, PIC, and CSv likely play a motor role in the egomotion signal processing, analyzing somatomotor signals, particularly from the lower limbs, together with visual egomotion signal to control (loco)motion.

### ACKNOWLEDGMENTS

The work was supported by the University of Foro Italico, grant to S.P. (CDR2.FFABR) and by PRIN 2015AWSW2Y to C.G.

### CONFLICT OF INTEREST

The authors declare no conflict of interest.

### ORCID

Sabrina Pitzalis  <https://orcid.org/0000-0002-4445-0391>

### REFERENCES

- Akselrod, M., Martuzzi, R., Serino, A., van der Zwaag, W., Gassert, R., & Blanke, O. (2017). Anatomical and functional properties of the foot and leg representation in areas 3b, 1 and 2 of primary somatosensory cortex in humans: A 7 T fMRI study. *NeuroImage*, 159, 473–487. <http://doi.org/10.1016/j.neuroimage.2017.06.021>
- Amiez, C., & Petrides, M. (2014). Neuroimaging evidence of the anatomofunctional organization of the human cingulate motor areas. *Cerebral Cortex*, 24(3), 563–578. <http://doi.org/10.1093/cercor/bhs329>
- Antal, A., Baudewig, J., Paulus, W., & Dechent, P. (2008). The posterior cingulate cortex and planum temporale/parietal operculum are activated by coherent visual motion. *Visual Neuroscience*, 25(1), 17–26. <http://doi.org/10.1017/S0952523808080024>

- Avanzini, P., Abdollahi, R. O., Sartori, I., Caruana, F., Pelliccia, V., Casaceli, G., ... Orban, G. A. (2016). Four-dimensional maps of the human somatosensory system. *Proceedings of the National Academy of Sciences of the United States of America*, 113(13), E1936–E1943. <https://doi.org/10.1073/pnas.1601889113>
- Bakola, S., Gamberini, M., Passarelli, L., Fattori, P., & Galletti, C. (2010). Cortical connections of parietal field PEC in the macaque: Linking vision and somatic sensation for the control of limb action. *Cerebral Cortex*, 20(11), 2592–2604. <http://doi.org/10.1093/cercor/bhq007>
- Bartels, A., Zeki, S., & Logothetis, N. K. (2008). Natural vision reveals regional specialization to local motion and to contrast-invariant, global flow in the human brain. *Cerebral Cortex*, 18(3), 705–717. <https://doi.org/10.1093/cercor/bhm107>
- Behzadi, Y., Restom, K., Liao, J., & Liu, T. T. (2007). A component based noise correction method (CompCor) for BOLD and perfusion based fMRI. *NeuroImage*, 37(1), 90–101. <http://doi.org/10.1016/j.neuroimage.2007.04.042>
- Billington, J., & Smith, A. T. (2015). Neural mechanisms for discounting head-roll-induced retinal motion. *Journal of Neuroscience*, 35(12), 4851–4856. <http://doi.org/10.1523/JNEUROSCI.3640-14.2015>
- Bremmer, F. (2011). Multisensory space: From eye-movements to self-motion. *The Journal of Physiology*, 589(4), 815–823. <http://doi.org/10.1113/jphysiol.2010.195537>
- Bremmer, F., Duhamel, J. R., Ben Hamed, S., & Graf, W. (2002). Heading encoding in the macaque ventral intraparietal area (VIP). *European Journal of Neuroscience*, 16(8), 1554–1568. <http://doi.org/10.1046/j.1460-9568.2002.02207.x>
- Bremmer, F., Schlack, A., Shah, N. J., Zafiris, O., Kubischik, M., Hoffmann, K. P., & Fink, G. R. (2001). Polymodal motion processing in posterior parietal and premotor cortex. *Neuron*, 29, 287–296. [http://doi.org/10.1016/S0896-6273\(01\)00198-2](http://doi.org/10.1016/S0896-6273(01)00198-2)
- Breviglieri, R., Galletti, C., Gamberini, M., Passarelli, L. A., & Fattori, P. (2006). Somatosensory cells in area PEC of macaque posterior parietal cortex. *Journal of Neuroscience*, 26(14), 3679–3684. <http://doi.org/10.1523/JNEUROSCI.4637-05.2006>
- Breviglieri, R., Galletti, C., Monaco, S., & Fattori, P. (2008). Visual, somatosensory, and bimodal activities in the macaque parietal area PEC. *Cerebral Cortex*, 18(4), 806–816. <http://doi.org/10.1093/cercor/bhm127>
- Brodmann, K. (1909). *Vergleichende Lokalisationslehre der Grosshirnrinde*, Barth, Leipzig: Germany. (Reprinted 1925).
- Buckner, R. L., Krienen, F. M., & Yeo, B. T. T. (2013). Opportunities and limitations of intrinsic functional connectivity MRI. *Nature Neuroscience*, 16(7), 832–837. <https://doi.org/10.1038/nn.3423>
- Byrne, P., Becker, S., & Burgess, N. (2007). Remembering the past and imagining the future: A neural model of spatial memory and imagery. *Psychological Review*, 114(2), 340–375. <http://doi.org/10.1037/0033-295X.114.2.340>
- Cardin, V., Sherrington, R., Hemsworth, L., & Smith, A. T. (2012). Human V6: Functional characterisation and localisation. *PLoS One*, 7(10), e47685. <http://doi.org/10.1371/journal.pone.0047685>
- Cardin, V., & Smith, A. T. (2010). Sensitivity of human visual and vestibular cortical regions to egomotion-compatible visual stimulation. *Cerebral Cortex*, 20(8), 1964–1973. <http://doi.org/10.1093/cercor/bhp268>
- Cardin, V., & Smith, A. T. (2011). Sensitivity of human visual cortical area V6 to stereoscopic depth gradients associated with self-motion. *Journal of Neurophysiology*, 106, 1240–1249. <http://doi.org/10.1152/jn.01120.2010>
- Cauda, F., Geminiani, G., D'agata, F., Duca, S., & Sacco, K. (2011). Discovering the somatotopic organization of the motor areas of the medial wall using low-frequency bold fluctuations. *Human Brain Mapping*, 32(10), 1566–1579. <http://doi.org/10.1002/hbm.21132>
- Chen, A., DeAngelis, G. C., & Angelaki, D. E. (2011a). Convergence of vestibular and visual self-motion signals in an area of the posterior sylvian fissure. *The Journal of Neuroscience: The Official Journal of the Society for Neuroscience*, 31(32), 11617–11627. <http://doi.org/10.1523/JNEUROSCI.1266-11.2011>
- Chen, A., DeAngelis, G. C., & Angelaki, D. E. (2011b). Representation of vestibular and visual cues to self-motion in ventral intraparietal cortex. *Journal of Neuroscience*, 31(33), 12036–12052. <http://doi.org/10.1523/JNEUROSCI.0395-11.2011>
- Chen, C. F., Kreutz-Delgado, K., Sereno, M. I., & Huang, R. S. (2017). Validation of periodic fMRI signals in response to wearable tactile stimulation. *NeuroImage*, 150, 99–111. <http://doi.org/10.1016/j.neuroimage.2017.02.024>
- Christensen, M. S., Lundbye-Jensen, J., Petersen, N., Geertsens, S. S., Paulson, O. B., & Nielsen, J. B. (2007). Watching your foot move—An fMRI study of visuomotor interactions during foot movement. *Cerebral Cortex*, 17(8), 1906–1917. <https://doi.org/10.1093/cercor/bhl101>
- Chumbley, J., Worsley, K., Flandin, G., & Friston, K. (2010). Topological FDR for neuroimaging. *NeuroImage*, 49, 3057–3064. <https://doi.org/10.1016/j.neuroimage.2009.10.090>
- Colby, C. L., Duhamel, J. R., & Goldberg, M. E. (1993). Ventral intraparietal area of the macaque: Anatomic location and visual response properties. *Journal of Neurophysiology*, 69(3), 902–914. <http://doi.org/10.1152/jn.1993.69.3.902>
- Corbetta, M., Miezin, F. M., Shulman, G. L., & Petersen, S. E. (1993). A PET study of visuospatial attention. *The Journal of Neuroscience: The Official Journal of the Society for Neuroscience*, 13(3), 1202–1226 Retrieved from <http://www.ncbi.nlm.nih.gov/pubmed/8441008>
- Cottureau, B. R., Smith, A. T., Rima, S., Fize, D., Héjja-Brichard, Y., Renaud, L., & Durand, J. B. (2017). Processing of egomotion-consistent optic flow in the rhesus macaque cortex. *Cerebral Cortex*, 27, 1–14. <http://doi.org/10.1093/cercor/bhw412>
- Crossland, M. D., Morland, A. B., Feely, M. P., Von Dem Hagen, E., & Rubin, G. S. (2008). The effect of age and fixation instability on retinotopic mapping of primary visual cortex. *Investigative Ophthalmology & Visual Science*, 49, 3734–3739. <https://doi.org/10.1167/iov.07-1621>
- Cunningham, D. A., Machado, A., Yue, G. H., Carey, J. R., & Plow, E. B. (2013). Functional somatotopy revealed across multiple cortical regions using a model of complex motor task. *Brain Research*, 1531, 25–36. <https://doi.org/10.1016/j.brainres.2013.07.050>
- Dale, A. M., Fischl, B., & Sereno, M. I. (1999). Cortical surface-based analysis: I. Segmentation and surface reconstruction. *NeuroImage*, 9(2), 179–194. <http://doi.org/10.1006/nimg.1998.0395>
- Dalla Volta, R., Fasano, F., Cerasa, A., Mangone, G., Quattrone, A., & Buccino, G. (2015). Walking indoors, walking outdoors: An fMRI study. *Frontiers in Psychology*, 6, 1–10. <http://doi.org/10.3389/fpsyg.2015.01502>
- Desikan, R. S., Ségonne, F., Fischl, B., Quinn, B. T., Dickerson, B. C., Blacker, D., ... Hyman, B. T. (2006). An automated labeling system for subdividing the human cerebral cortex on MRI scans into gyral based regions of interest. *NeuroImage*, 31, 968–980. <https://doi.org/10.1016/j.neuroimage.2006.01.021>
- Di Russo, F., Pitzalis, S., & Spinelli, D. (2003). Fixation stability and saccadic latency in elite shooters. *Vision Research*, 43(17), 1837–1845. [http://doi.org/10.1016/S0042-6989\(03\)00299-2](http://doi.org/10.1016/S0042-6989(03)00299-2)
- Di Russo, F., Committeri, G., Pitzalis, S., Spitoni, G., Piccardi, L., Galati, G., ... Pizzamiglio, L. (2006). Cortical plasticity following surgical extension of lower limbs. *NeuroImage*, 30, 172–183.
- Duffy, C. J. (1998). MST neurons respond to optic flow and translational movement. *Journal of Neurophysiology*, 80(4), 1816–1827. <https://doi.org/10.1152/jn.1998.80.4.1816>
- Duhamel, J. R., Colby, C. L., & Goldberg, M. E. (1998). Ventral intraparietal area of the macaque: Congruent visual and somatic response properties. *Journal of Neurophysiology*, 79(1), 126–136. <http://doi.org/10.1234/12345678>
- Dukelow, S. P., DeSouza, J. F. X., Culham, J. C., van den Berg, A. V., Menon, R. S., & Vilis, T. (2001). Distinguishing subregions of the human MT+ complex using visual fields and pursuit eye movements. *Journal of Neurophysiology*, 86(4), 1991–2000. <http://doi.10.1152/jn.2001.86.4.1991>

- Eger, E., Pinel, P., Dehaene, S., & Kleinschmidt, A. (2015). Spatially invariant coding of numerical information in functionally defined subregions of human parietal cortex. *Cerebral Cortex*, 25, 1319–1329. <https://doi.org/10.1093/cercor/bht323>
- Eickhoff, S. B., Amunts, K., Mohlberg, H., & Zilles, K. (2006). The human parietal operculum. II. Stereotaxic maps and correlation with functional imaging results. *Cerebral Cortex*, 16(2), 268–279. <http://doi.org/10.1093/cercor/bhi106>
- Eickhoff, S. B., Weiss, P. H., Amunts, K., Fink, G. R., & Zilles, K. (2005). Identifying human parieto-insular vestibular cortex using fMRI and cytoarchitectonic mapping. *Human Brain Mapping*, 27(7), 611–621. <http://doi.org/10.1002/hbm.20205>
- Epstein, R. A. (2008). Parahippocampal and retrosplenial contributions to human spatial navigation. *Trends in Cognitive Sciences*, 12(10), 388–396. <http://doi.org/10.1016/j.tics.2008.07.004>
- Epstein, R. A., & Kanwisher, N. (1998). A cortical representation of the local visual environment. *Nature*, 392(6676), 598–601. <http://doi.org/10.1038/33402>
- Fasold, O., von Brevern, M., Kuhberg, M., Ploner, C. J., Villringer, A., Lempert, T., & Wenzel, R. (2002). Human vestibular cortex as identified with caloric stimulation in functional magnetic resonance imaging. *NeuroImage*, 17(3), 1384–1393. <http://doi.org/10.1006/nimg.2002.1241>
- Field, D. T., Inman, L. A., & Li, L. (2015). Visual processing of optic flow and motor control in the human posterior cingulate sulcus. *Cortex*, 71, 377–389. <http://doi.org/10.1016/j.cortex.2015.07.014>
- Filimon, F., Nelson, J. D., Hagler, D. J., & Sereno, M. I. (2007). Human cortical representations for reaching: Mirror neurons for execution, observation, and imagery. *NeuroImage*, 37(4), 1315–1328. <https://doi.org/10.1016/j.neuroimage.2007.06.008>
- Filimon, F., Nelson, J. D., Huang, R. S., & Sereno, M. I. (2009). Multiple parietal reach regions in humans: Cortical representations for visual and proprioceptive feedback during on-line reaching. *The Journal of Neuroscience*, 29, 2961–2971. <https://doi.org/10.1523/JNEUROSCI.3211-08.2009>
- Fischer, E., Bühlhoff, H. H., Logothetis, N. K., & Bartels, A. (2012a). Human areas V3A and V6 compensate for self-induced planar visual motion. *Neuron*, 73(6), 1228–1240. <http://doi.org/10.1016/j.neuron.2012.01.022>
- Fischer, E., Bühlhoff, H. H., Logothetis, N. K., & Bartels, A. (2012b). Visual motion responses in the posterior cingulate sulcus: A comparison to V5/MT and MST. *Cerebral Cortex*, 22(4), 865–876. <http://doi.org/10.1093/cercor/bhr154>
- Fischl, B., Sereno, M. I., & Dale, A. M. (1999). Cortical surface-based analysis: II. Inflation, flattening, and a surface-based coordinate system. *NeuroImage*, 9(2), 195–207. <http://doi.org/10.1006/nimg.1998.0396>
- Fischl, B., Sereno, M. I., Tootell, R. B. H., & Dale, A. M. (1999). High-resolution intersubject averaging and a coordinate system for the cortical surface. *Human Brain Mapping*, 8, 272–284. [https://doi.org/10.1002/\(SICI\)1097-0193\(1999\)8:4<272::AID-HBM10>3.0.CO;2-4](https://doi.org/10.1002/(SICI)1097-0193(1999)8:4<272::AID-HBM10>3.0.CO;2-4)
- Fox, M. D., & Raichle, M. E. (2007). Spontaneous fluctuations in brain activity observed with functional magnetic resonance imaging. *Nature Reviews Neuroscience*, 8(9), 700–711. <http://doi.org/10.1038/nrn2201>
- Frank, S. M., Baumann, O., Mattingley, J. B., & Greenlee, M. W. (2014). Vestibular and visual responses in human posterior insular cortex. *Journal of Neurophysiology*, 112(10), 2481–2491. <http://doi.org/10.1152/jn.00078.2014>
- Frank, S. M., Sun, L., Forster, L., Peter, U. T., & Greenlee, M. W. (2016). Cross-modal attention effects in vestibular cortex during attentive tracking of moving objects. *The Journal of Neuroscience*, 36(50), 12720–12728. <http://doi.org/10.1523/JNEUROSCI.2480-16.2016>
- Frank, S. M., Wirth, A. M., & Greenlee, M. W. (2016). Visual-vestibular processing in the human sylvian fissure. *Journal of Neurophysiology*, 116(2), 263–271. <http://doi.org/10.1152/jn.00009.2016>
- Fried, I., Katz, A., McCarthy, G., Sass, K. J., Williamson, P., Spencer, S. S., & Spencer, D. D. (1991). Functional organization of human supplementary motor cortex studied by electrical stimulation. *The Journal of Neuroscience: The Official Journal of the Society for Neuroscience*, 11(11), 3656–3666. <https://doi.org/10.1523/JNEUROSCI.11-11-03656.1991>
- Furlan, M., Wann, J. P., & Smith, A. T. (2014). A representation of changing heading direction in human cortical areas pVIP and CSv. *Cerebral Cortex*, 24(11), 2848–2858. <http://doi.org/10.1093/cercor/bht132>
- Galletti, C., Battaglini, P. P., & Fattori, P. (1990). “Real-motion” cells in area V3A of macaque visual cortex. *Experimental Brain Research*, 82(1), 67–76. <http://doi.org/10.1007/BF00230838>
- Galletti, C., & Fattori, P. (2003). Neuronal mechanisms for detection of motion in the field of view. *Neuropsychologia*, 41(13), 1717–1727. [http://doi.org/10.1016/S0028-3932\(03\)00174-X](http://doi.org/10.1016/S0028-3932(03)00174-X)
- Galletti, C., & Fattori, P. (2018). The dorsal visual stream revisited: Stable circuits or dynamic pathways? *Cortex*, 98, 1–15. <http://doi.org/10.1016/j.cortex.2017.01.009>
- Gamberini, M., Dal Bò, G., Breveglieri, R., Briganti, S., Passarelli, L., Fattori, P., & Galletti, C. (2018). Sensory properties of the caudal aspect of the macaque's superior parietal lobule. *Brain Structure and Function*, 223(4), 1863–1879. <https://doi.org/10.1007/s00429-017-1593-x>
- Gibson, J. J. (1950). *The perception of the visual world*. Boston, MA: Houghton Mifflin.
- Gitelman, D. R., Nobre, A. C., Parrish, T. B., LaBar, K. S., Kim, Y. H., Meyer, J. R., & Mesulam, M. M. (1999). A large-scale distributed network for covert spatial attention. *Brain*, 122(6), 1093–1106. <https://doi.org/10.1093/brain/122.6.1093>
- Glasser, M. F., Sotiropoulos, S. N., Wilson, J. A., Coalson, T. S., Fischl, B., Andersson, J. L., ... WU-Minn HCP Consortium. (2013). The minimal preprocessing pipelines for the Human Connectome Project. *NeuroImage*, 80, 105–124. <http://doi.org/10.1016/j.neuroimage.2013.04.127>
- Graziano, M. S. A., & Cooke, D. F. (2006). Parieto-frontal interactions, personal space, and defensive behavior. *Neuropsychologia*, 44(13), 2621–2635. <http://doi.org/10.1016/j.neuropsychologia.2005.09.011>
- Greenlee, M. W., Frank, S. M., Kaliuzhna, M., Blanke, O., Bremmer, F., Churan, J., ... Smith, A. T. (2016). Multisensory integration in self motion perception. *Multisensory Research*, 29(6–7), 525–556. <https://doi.org/10.1163/22134808-00002527>
- Guldin, W. O., & Grüsser, O. J. (1998). Is there a vestibular cortex? *Trends in Neurosciences*, 21(6), 254–259. [http://doi.org/10.1016/S0166-2236\(97\)01211-3](http://doi.org/10.1016/S0166-2236(97)01211-3)
- Heed, T., Beurze, S. M., Toni, I., Röder, B., & Medendorp, W. P. (2011). Functional rather than effector-specific organization of human posterior parietal cortex. *The Journal of Neuroscience: The Official Journal of the Society for Neuroscience*, 31(8), 3066–3076. <http://doi.org/10.1523/JNEUROSCI.4370-10.2011>
- Heed, T., Leoné, F. T. M., Toni, I., & Medendorp, W. P. (2016). Functional versus effector-specific organization of the human posterior parietal cortex: Revisited. *Journal of Neurophysiology*, 116(4), 1885–1899. <http://doi.org/10.1152/jn.00312.2014>
- Huang, R. S., Chen, C., & Sereno, M. I. (2017). Mapping the complex topological organization of the human parietal face area. *NeuroImage*, 163, 459–470. <http://doi.org/10.1016/j.neuroimage.2017.09.004>
- Huang, R. S., Chen, C., Tran, A. T., Holstein, K. L., & Sereno, M. I. (2012). Mapping multisensory parietal face and body areas in humans. *Proceedings of the National Academy of Sciences of the United States of America*, 109(44), 18114–18119. <http://doi.org/10.1073/pnas.1207946109>
- Huang, R. S., Chen, C. F., & Sereno, M. I. (2015). Neural substrates underlying the passive observation and active control of translational egomotion. *The Journal of Neuroscience*, 35(10), 4258–4267. <https://doi.org/10.1523/JNEUROSCI.2647-14.2015>
- Huang, R. S., & Sereno, M. I. (2013). Bottom-up retinotopic organization supports top-down mental imagery. *The Open Neuroimaging Journal*, 7 (858), 58–67. <http://doi.org/10.2174/1874440001307010058>



- Huang, R. S., & Sereno, M. I. (2018). Multisensory and sensorimotor maps. *Handbook of Clinical Neurology*, 151, 141–161. <https://doi.org/10.1016/B978-0-444-63622-5.00007-3>
- Kapreli, E., Athanasopoulos, S., Paphanasiou, M., Van Hecke, P., Kelekis, D., Peeters, R., & Sunaert, S. (2008). Lower limb sensorimotor network: Issues of somatotopy and overlap. *Cortex*, 43(2), 219–232. [http://doi.org/10.1016/S0010-9452\(08\)70477-5](http://doi.org/10.1016/S0010-9452(08)70477-5)
- Kim, Y.-H., Gitelman, D. R., Nobre, A. C., Parrish, T. B., LaBar, K. S., & Mesulam, M.-M. (1999). The large-scale neural network for spatial attention displays multifunctional overlap but differential asymmetry. *NeuroImage*, 9(3), 269–277. <http://doi.org/10.1006/nimg.1999.0408>
- Koenderink, J. J., & Physics, P. (1986). Optic flow. *Vision Research*, 26(1), 161–179. [http://doi.org/10.1016/0042-6989\(86\)90078-7](http://doi.org/10.1016/0042-6989(86)90078-7)
- Kolster, H., Peeters, R., & Orban, G. A. (2010). The retinotopic organization of the human middle temporal area MT/V5 and its cortical neighbors. *Journal of Neuroscience*, 30(29), 9801–9820. <http://doi.org/10.1523/JNEUROSCI.2069-10.2010>
- Korkmaz Hacialihafiz, D., & Bartels, A. (2015). Motion responses in scene-selective regions. *NeuroImage*, 118, 438–444. <https://doi.org/10.1016/j.neuroimage.2015.06.031>
- Kwong, K. K., Belliveau, J. W., Chesler, D. A., Goldberg, I. E., Weisskoff, R. M., Poncelet, B. P., & Turner, R. (1992). Dynamic magnetic resonance imaging of human brain activity during primary sensory stimulation. *Proceedings of the National Academy of Sciences of the United States of America*, 89(12), 5675–5679. <http://doi.org/10.1073/pnas.89.12.5675>
- Leoné, F. T. M., Heed, T., Toni, I., & Medendorp, W. P. (2014). Understanding effector selectivity in human posterior parietal cortex by combining information patterns and activation measures. *Journal of Neuroscience*, 34(21), 7102–7112. <http://doi.org/10.1523/JNEUROSCI.5242-13.2014>
- Lorey, B., Naumann, T., Pilgramm, S., Petermann, C., Bischoff, M., Zentgraf, K., ... Munzert, J. (2013). How equivalent are the action execution, imagery, and observation of intransitive movements? Revisiting the concept of somatotopy during action simulation. *Brain and Cognition*, 81(1), 139–150. <https://doi.org/10.1016/j.bandc.2012.09.011>
- Luft, A. R., Smith, G. V., Forrester, L., Whittall, J., Macko, R. F., Hauser, T. K., ... Hanley, D. F. (2002). Comparing brain activation associated with isolated upper and lower limb movement across corresponding joints. *Human Brain Mapping*, 17(2), 131–140. <https://doi.org/10.1002/hbm.10058>
- Mangan, A. P., & Whitaker, R. T. (1999). Partitioning 3D surface meshes using watershed segmentation. *IEEE Transactions on Visualization and Computer Graphics*, 5(4), 308–321. <http://doi.org/10.1109/2945.817348>
- Margulies, D. S., Vincent, J. L., Kelly, C., Lohmann, G., Uddin, L. Q., Biswal, B. B., & Petrides, M. (2009). Precuneus shares intrinsic functional architecture in humans and monkeys. *Proceedings of the National Academy of Sciences of the United States of America*, 106(47), 20069–20074. <http://doi.org/10.1073/pnas.0905314106>
- Marigold, D. S. (2008). Role of peripheral visual cues in online visual guidance of locomotion. *Exercise and Sport Sciences Reviews*, 36(3), 145–151. <http://doi.org/10.1097/JES.0b013e31817bff72>
- Mesulam, M. M. (1999). Spatial attention and neglect: Parietal, frontal and cingulate contributions to the mental representation and attentional targeting of salient extrapersonal events. *Philosophical Transactions of the Royal Society B: Biological Sciences*, 354(1387), 1325–1346. <http://doi.org/10.1098/rstb.1999.0482>
- Mikellidou, K., Kurzawski, J. W., Frijia, F., Montanaro, D., Greco, V., Burr, D. C., & Morrone, M. C. (2017). Area prostriata in the human brain. *Current Biology*, 27(19), 3056–3060.e3. <http://doi.org/10.1016/j.cub.2017.08.065>
- Morrone, M. C., Tosetti, M., Montanaro, D., Fiorentini, A., Cioni, G., & Burr, D. C. (2000). A cortical area that responds specifically to optic flow, revealed by fMRI. *Nature Neuroscience*, 3(12), 1322–1328. <http://doi.org/10.1038/81860>
- Oldfield, R. C. (1971). The assessment and analysis of handedness: The Edinburgh inventory. *Neuropsychologia*, 9, 97–113. [https://doi.org/10.1016/0028-3932\(71\)90067-4](https://doi.org/10.1016/0028-3932(71)90067-4)
- Pandya, D. N., & Seltzer, B. (1982). Intrinsic connections and architectonics of posterior parietal cortex in the rhesus monkey. *Journal of Comparative Neurology*, 204(2), 196–210. <http://doi.org/10.1002/cne.902040208>
- Paus, T. (1996). Location and function of the human frontal eye-field: A selective review. *Neuropsychologia*, 34(6), 475–483. [http://doi.org/10.1016/0028-3932\(95\)00134-4](http://doi.org/10.1016/0028-3932(95)00134-4)
- Picard, N., & Strick, P. L. (1996). Motor areas of the medial wall: A review of their location and functional activation. *Cerebral Cortex*, 6(3), 342–353. <http://doi.org/10.1093/cercor/6.3.342>
- Pitzalis, S., Bozzacchi, C., Bultrini, A., Fattori, P., Galletti, C., & Di Russo, F. (2013). Parallel motion signals to the medial and lateral motion areas V6 and MT+. *NeuroImage*, 67, 89–100. <http://doi.org/10.1016/j.neuroimage.2012.11.022>
- Pitzalis, S., Fattori, P., & Galletti, C. (2013). The functional role of the medial motion area V6. *Frontiers in Behavioral Neuroscience*, 6, 91. <http://doi.org/10.3389/fnbeh.2012.00091>
- Pitzalis, S., Galletti, C., Huang, R. S., Patria, F., Committeri, G., Galati, G., & Sereno, M. I. (2006). Wide-field retinotopy defines human cortical visual area V6. *Journal of Neuroscience*, 26(30), 7962–7973. <http://doi.org/10.1523/JNEUROSCI.0178-06.2006>
- Pitzalis, S., Sdoia, S., Bultrini, A., Committeri, G., Di Russo, F., Fattori, P., & Galati, G. (2013). Selectivity to translational egomotion in human brain motion areas. *PLoS One*, 8(4), 1–14. <http://doi.org/10.1371/journal.pone.0060241>
- Pitzalis, S., Sereno, M. I., Committeri, G., Fattori, P., Galati, G., Patria, F., & Galletti, C. (2010). Human V6: The medial motion area. *Cerebral Cortex*, 20(2), 411–424. <http://doi.org/10.1093/cercor/bhp112>
- Pitzalis, S., Sereno, M. I., Committeri, G., Fattori, P., Galati, G., Tosoni, a., & Galletti, C. (2013). The human homologue of macaque area V6A. *NeuroImage*, 82, 517–530. <http://doi.org/10.1016/j.neuroimage.2013.06.026>
- Pitzalis, S., Strappini, F., De Gasperis, M., Bultrini, A., & Di Russo, F. (2012). Spatio-temporal brain mapping of motion-onset VEPs combined with fMRI and retinotopic maps. *PLoS One*, 7(4), e35771. <http://doi.org/10.1371/journal.pone.0035771>
- Rocca, M. A., & Filippi, M. (2010). FMRI correlates of execution and observation of foot movements in left-handers. *Journal of the Neurological Sciences*, 288(1–2), 34–41. <https://doi.org/10.1016/j.jns.2009.10.013>
- Rubén, J., Schwiemann, J., Deuchert, M., Meyer, R., Krause, T., Curio, G., & Villringer, A. (2001). Somatotopic organization of human secondary somatosensory cortex. *Cerebral Cortex*, 11(5), 463–473. <http://doi.org/10.1093/cercor/11.5.463>
- Rushton, S. K., Niehorster, D. C., Warren, P. A., & Li, L. (2018). The primary role of flow processing in the identification of scene-relative object movement. *Journal of Neuroscience*, 38(7), 1737–1743. <https://doi.org/10.1523/JNEUROSCI.3530-16.2017>
- Sahyoun, C., Floyer-Lea, A., Johansen-Berg, H., & Matthews, P. M. (2004). Towards an understanding of gait control: Brain activation during the anticipation, preparation and execution of foot movements. *NeuroImage*, 21(2), 568–575. <https://doi.org/10.1016/j.neuroimage.2003.09.065>
- Schindler, A., & Bartels, A. (2016). Motion parallax links visual motion areas and scene regions. *NeuroImage*, 125, 803–812. <http://doi.org/10.1016/j.neuroimage.2015.10.066>
- Sereno, M. I., & Huang, R. S. (2006). A human parietal face area contains aligned head-centered visual and tactile maps. *Nature Neuroscience*, 9(10), 1337–1343. <http://doi.org/10.1038/nn1777>
- Sereno, M. I., Pitzalis, S., & Martinez, A. (2001). Mapping of contralateral space in retinotopic coordinates by a parietal cortical area in humans. *Science*, 294(5545), 1350–1354. <http://doi.org/10.1126/science.1063695>
- Sherrill, K. R., Chrastil, E. R., Ross, R. S., Erdem, U. M., Hasselmo, M. E., & Stern, C. E. (2015). Functional connections between optic flow areas and navigationally responsive brain regions during goal-directed

- navigation. *NeuroImage*, 118, 386–396. <http://doi.org/10.1016/j.neuroimage.2015.06.009>
- Smith, A. T., Beer, A. L., Furlan, M., & Mars, R. B. (2017). Connectivity of the cingulate sulcus visual area (CSv) in the human cerebral cortex. *Cerebral Cortex*, 28(2), 713–772. <http://doi.org/10.1093/cercor/bhx002>
- Smith, A. T., Greenlee, M. W., DeAngelis, G. C., & Angelaki, D. (2017). Distributed visual-vestibular processing in the cerebral cortex of man and macaque. *Multisensory Research*, 30(2), 91–120. <https://doi.org/10.1163/22134808-00002568>
- Smith, A. T., Wall, M. B., & Thilo, K. V. (2012). Vestibular inputs to human motion-sensitive visual cortex. *Cerebral Cortex*, 22(5), 1068–1077. <http://doi.org/10.1093/cercor/bhr179>
- Smith, A. T., Wall, M. B., Williams, A. L., & Singh, K. D. (2006). Sensitivity to optic flow in human cortical areas MT and MST. *European Journal of Neuroscience*, 23(2), 561–569. <http://doi.org/10.1111/j.1460-9568.2005.04526.x>
- Strappini, F., Gilboa, E., Pitzalis, S., Kay, K., McAvoy, M., Nehorai, A., & Snyder, A. Z. (2017). Adaptive smoothing based on Gaussian processes regression increases the sensitivity and specificity of fMRI data. *Human Brain Mapping*, 38(3), 1438–1459. <http://doi.org/10.1002/hbm.23464>
- Strappini, F., Pitzalis, S., Snyder, A. Z., McAvoy, M. P., Sereno, M. I., Corbetta, M., & Shulman, G. L. (2015). Eye position modulates retinotopic responses in early visual areas: A bias for the straight-ahead direction. *Brain Structure and Function*, 220(5), 2587–2601. <http://doi.org/10.1007/s00429-014-0808-7>
- Sulpizio, V., Boccia, M., Guariglia, C., & Galati, G. (2016). Functional connectivity between posterior hippocampus and retrosplenial complex predicts individual differences in navigational ability. *Hippocampus*, 26(7), 841–847. <http://doi.org/10.1002/hipo.22592>
- Sulpizio, V., Committeri, G., & Galati, G. (2014). Distributed cognitive maps reflecting real distances between places and views in the human brain. *Frontiers in Human Neuroscience*, 8, 716. <http://doi.org/10.3389/fnhum.2014.00716>
- Sulpizio, V., Committeri, G., Lambrey, S., Berthoz, A., & Galati, G. (2013). Selective role of lingual/parahippocampal gyrus and retrosplenial complex in spatial memory across viewpoint changes relative to the environmental reference frame. *Behavioural Brain Research*, 242, 62–75. <http://doi.org/10.1016/j.bbr.2012.12.031>
- Tal, Z., Geva, R., & Amedi, A. (2017). Positive and negative somatotopic BOLD responses in contralateral versus ipsilateral penfield homunculus. *Cerebral Cortex*, 27(2), 962–980. <http://doi.org/10.1093/cercor/bhx024>
- Tootell, R. B., Mendola, J. D., Hadjikhani, N. K., Ledden, P. J., Liu, A. K., Reppas, J. B., & Dale, A. M. (1997). Functional analysis of V3A and related areas in human visual cortex. *The Journal of Neuroscience: The Official Journal of the Society for Neuroscience*, 17(18), 7060–7078. <https://doi.org/10.1523/JNEUROSCI.17-18-07060.1997>
- Tosoni, A., Galati, G., Romani, G. L., & Corbetta, M. (2008). Sensory-motor mechanisms in human parietal cortex underlie arbitrary visual decisions. *Nature Neuroscience*, 11(12), 1446–1453. <http://doi.org/10.1038/nn.2221>
- Tosoni, A., Pitzalis, S., Committeri, G., Fattori, P., Galletti, C., & Galati, G. (2015). Resting-state connectivity and functional specialization in human medial parieto-occipital cortex. *Brain Structure and Function*, 220(6), 3307–3321. <http://doi.org/10.1007/s00429-014-0858-x>
- Uddin, L. Q. (2010). Typical and atypical development of functional human brain networks: Insights from resting-state fMRI. *Frontiers in Systems Neuroscience*, 4, 1–12. <http://doi.org/10.3389/fnsys.2010.0002>
- Uesaki, M., & Ashida, H. (2015). Optic-flow selective cortical sensory regions associated with self-reported states ofvection. *Frontiers in Psychology*, 6, 775. <https://doi.org/10.3389/fpsyg.2015.00775>
- Van Essen, D. C., Glasser, M. F., Dierker, D. L., Harwell, J., & Coalson, T. (2011). Parcellations and hemispheric asymmetries of human cerebral cortex analyzed on surface-based atlases. *Cerebral Cortex*, 22(10), 2241–2262. <http://doi.org/10.1093/cercor/bhr291>
- Van Essen, D. C., Glasser, M. F., Dierker, D. L., Harwell, J., & Coalson, T. (2012). Parcellations and hemispheric asymmetries of human cerebral cortex analyzed on surface-based atlases. *Cerebral Cortex*, 22, 2241–2262. <https://doi.org/10.1093/cercor/bhr291>
- Vogt, B. A., Vogt, L., & Laureys, S. (2006). Cytology and functionally correlated circuits of human posterior cingulate areas. *NeuroImage*, 29(2), 452–466. <http://doi.org/10.1016/j.neuroimage.2005.07.048>
- Wada, A., Sakano, Y., & Ando, H. (2016). Differential responses to a visual self-motion signal in human medial cortical regions revealed by wide-view stimulation. *Frontiers in Psychology*, 7, 1–17. <http://doi.org/10.3389/fpsyg.2016.00309>
- Wall, M. B., & Smith, A. T. (2008). The representation of egomotion in the human brain. *Current Biology*, 18(3), 191–194. <http://doi.org/10.1016/j.cub.2007.12.053>
- Warren, P. A., & Rushton, S. K. (2009). Optic flow processing for the assessment of object movement during ego movement. *Current Biology*, 19(18), 1555–1560. <http://doi.org/10.1016/j.cub.2009.07.057>
- Zhang, S., & Li, C.-S. R. (2012). Functional connectivity mapping of the human precuneus by resting state fMRI. *NeuroImage*, 59(4), 3548–3562. <http://doi.org/10.1016/j.neuroimage.2011.11.023>
- Zlatkina, V., Amiez, C., & Petrides, M. (2016). The postcentral sulcal complex and the transverse postcentral sulcus and their relation to sensorimotor functional organization. *European Journal of Neuroscience*, 43(10), 1268–1283. <http://doi.org/10.1111/ejn.13049>

**How to cite this article:** Serra C, Galletti C, Di Marco S, et al. Egomotion-related visual areas respond to active leg movements. *Hum Brain Mapp.* 2019;40:3174–3191. <https://doi.org/10.1002/hbm.24589>